Fall 2019

Numerical Modeling of Shoreline Response to Storm Tides and Sea Level Rise

Akash Sahu
Old Dominion University, asahu001@odu.edu

NUMERICAL MODELING OF SHORELINE RESPONSE TO STORM TIDES AND SEA LEVEL RISE

by

Akash Sahu
B. Tech. May 2015, Motilal Nehru National Institute of Technology Allahabad, India

A Thesis Submitted to the Faculty of
Old Dominion University in Partial Fulfillment of the
Requirements for the Degree of

MASTER OF SCIENCE

CIVIL ENGINEERING

OLD DOMINION UNIVERSITY
December 2019

Approved by:

Navid Tahvildari (Director)

Gangfeng Ma (Member)

Jaewan Yoon (Member)

ABSTRACT

NUMERICAL MODELING OF SHORELINE RESPONSE TO STORM TIDES AND SEA LEVEL RISE

Akash Sahu
Old Dominion University, 2019
Director: Dr. Navid Tahvildari

In this study, an integrated hydrodynamic, wave, and sediment transport modeling approach is developed for predicting the spatiotemporal variation of erosion of a sandy shoreline due to storm surge, wave action, tidal variations, and relative sea level rise (RSLR). The study site is located at the northern most portion of the city of Norfolk, Virginia, and it is of importance to the city, both in terms of tourism and for the protection that it provides for upland properties against storms. The region, in general, experiences the highest rate of RSLR on the U.S. East Coast which should result in high rate of erosion. The stretch of the shoreline that is of particular interest in this study has documented high erosion rates and undergoes frequent re-nourishment. Future beach nourishment and re-nourishment projects can benefit from long-term data on beach morphological change and reliable models to predict erosion in response to changing coastal forces. This study aims to develop a reliable predictive model, closely integrated with available field surveys, for shoreline erosion. A coupled hydrodynamic+wave model, based on the Delft3D modeling suite, is developed and applied to compute flow and wave parameters for the area of interest. Upon validation of the coupled model with in-situ water level and wave data, the model output is used as input to the XBeach model, which computes the shoreline response for a two-dimensional grid along the beach. The XBeach model is validated with field surveys. The model is then applied to assess RSLR impacts on beach erosion. RSLR scenarios span

moderate to high projections, and three time horizons of 2020, 2030 and 2070 are considered. The results indicate that RSLR consistently increases shoreline erosion along the beach.

ACKNOWLEDGEMENTS

I would like to express my gratitude to my advisor, Dr. Navid Tahvildari, for giving me the opportunity to do my research under his guidance at Old Dominion University. I would also like to thank my friends and family who have supported me and have been a constant source of encouragement throughout my journey.

This research was supported by grants from the Department of Transportation's Mid-Atlantic Transportation Sustainability-University Transportation Center (MATS-UTC) and from the Commonwealth Center for Recurrent Flooding Resiliency (CCRFR).

TABLE OF CONTENTS

Page

LIST OF TABLES vii

LIST OF FIGURES viii

Chapter

1. INTRODUCTION 1

2. LITERATURE REVIEW 4

3. STUDY AREA 7

4. METHODOLOGY 10
- 4.1 Modeling Framework 10
- 4.2 Model Set-up and Governing Equations 12
  - 4.2.1 Delft3D-FLOW Model 12
  - 4.2.2 Delft3D-WAVE Model 13
  - 4.2.3 Coupling of Flow and Wave Models 14
  - 4.2.3.1 Grid Generation 16
  - 4.2.3.2 Boundary Conditions 18
  - 4.2.3.2.1 Tides and Wind Forcing 19
  - 4.2.3.2.2 Topographic and Bathymetric Data 20
  - 4.2.4 XBeach Model 21
  - 4.2.4.1 Grid Generation 22
  - 4.2.4.2 Boundary Conditions 22
- 4.3 Relative Sea Level Rise 24

5. RESULTS 25
- 5. 1 Calibration and Validation 25
  - 5.1.1 Flow-Wave Coupled Model 25
  - 5.1.2 XBeach Model 31
- 5.2 Water Level and Significant Wave Height under Future RSLR Scenarios 34
- 5.3 Erosion under Future RSLR Scenarios 35
- 5.4 Shoreline Recession under Future RSLR Scenarios 37

6. CONCLUSIONS AND DISCUSSION 39

7. RECOMMENDATIONS 42

Page

REFERENCES 44

VITA 50

LIST OF TABLES

Table Page

1. RSLR scenarios used in FLOW +WAVE simulations. The values are based on NOAA Technical Report NOS CO-OPS 083 (Sweet et al., 2017). 24

2. Final values of calibration parameters. 25

3. Observation points for Grid 1 and Grid 2. 26

4. Error statistics of Grid 1 model parameters for the selected locations. 29

5. Error statistics of Grid 2 model parameters for the selected locations. 30

6. Brier Skill Score (BSS) for three cross-shore profiles. 32

7. Increase in maximum water level and significant wave height from 2011 at the boundary of each transect for 3 RSLR scenarios. 35

8. Calculated erosion in m (m^3/m^2) along the transects for the 3 high RSLR scenarios for the 3 model years. 35

9. Shoreline recession in meters at the three transects for five RSLR scenarios. 38

LIST OF FIGURES

Figure Page

1. Location of Willoughby Spit-Ocean View Beach in Norfolk. 3

2. View of extent of study area. 9

3. Schematic view of modeling framework. 11

4.(a) Boundaries of Grid 1 domain and (b) Grid 1 projected on a segment of the study area. 17

5.(a) Boundaries of Grid 2 domain and (b) Grid 2 projected on a segment of the study area. 18

6. View of Grid 1 and Grid 2 set-up in domain decomposition mode. 18

7. View of boundary conditions (a) contour plot of equidistant wind forcing in m/s and (b) contour plot of topographic/bathymetric data. 20

8. (a) Boundaries of XBeach domain and (b) Computational grid projected on a segment of the study area. 22

9. Plan view of topographic/bathymetric transects survey. 23

10. Locations of tide and wave gauges used for model calibration and validation. 28

11. Model validation for Grid 1 observation points with in-situ measured data(a) Water level comparison (b) Significant wave height comparison (c) Mean wave period comparison and (d) Mean wave direction comparison. 29

12. Model validation for Grid 2 observation points with in-situ measured data (a) Water level comparison (b) Significant wave height comparison (c) Mean wave period comparison and (d) Mean wave direction comparison. 30

13. Location of cross-shore profiles used for XBeach model validation. 33

14. Comparison of calculated profile vs measured pre and post storm profiles for the three cross-shore profiles. 33

15. Variation of hydrodynamics with RSLR at offshore boundary of the XBeach transects (a) Maximum Water Level variation (b) Maximum Significant Wave Height variation. 34

Figure Page

16. Plot of erosion in m (m^3/m^2) along the three transects for the 9 RSLR scenarios. 36

17. Variation of erosion hotspot along Transect 3 for baseline case and two RSLR scenarios.... 37

18. Shoreline recession at Transect 3 for the year 2070 due to storm induced erosion and high (H) RSLR. 38

CHAPTER 1

INTRODUCTION

Hurricanes have been the costliest natural hazard in the U.S. and their increase in intensity and frequency, due to climate change (Emanuel, 1987, 2008; Bender et al., 2010) and relative sea level rise (RSLR), will exacerbate the vulnerability of coastal region (Irish et al., 2009). Coastal shorelines are highly prone to storm waves and rising sea levels, and they are in constant states of change (Enríquez et al., 2017). Storm events, especially, amplify coastal erosion due to severe hydrodynamic conditions which can eventually lead to the failure of coastal dune systems. Human activity, such as agriculture and development, also drastically accelerates the natural rate of shoreline change (Virginia Department of Conservation and Recreation, 2019). Beach erosion has become a universal problem, as it has been estimated that 70% of all the beaches in the world are eroding (Bird, 1985). The erosion problem is more extensive in some areas that others; for example, some Virginia shorelines have historic erosion rates of up to 30 feet per year (Virginia Department of Conservation and Recreation, 2019).

Shoreline change can create a lot of potential problems. If left unmanaged, it can cause a drop in property values, loss of productive land and, in the worst cases, injury or loss of life. There are also negative impacts to water quality from shoreline erosion. Fine soil particles (silt and clay) can cloud the water column and reduce the amount of sunlight that reaches the bottom. Decreased sunlight greatly reduces the abundance of submerged aquatic vegetation, which provides a critical habitat for juvenile fish and crabs. Along with sediment, eroding shorelines also contribute nutrients, such as nitrogen and phosphorus, which naturally occur in soil, to the receiving water body. Excessive amounts of these elements can cause algal blooms and greatly

lower the amount of dissolved oxygen in the water which, in turn, can cause fish kills (Virginia Department of Conservation and Recreation, 2019).

It is projected that nearly half the U.S. population will live in coastal counties by 2020 (NOAA, 2019). As the population is growing more rapidly in the coastal zone than in any other segment of the nation, the stresses on utilization of the shorelines have also increased. Since these stresses may become more severe, there is a need for planning and management of the utilization of limited coastal resources. Without planning, the very elements which attract people to the shore may be destroyed by incompatible utilization. Any attempt to handle coastal management problems, either to arrest erosion or prevent deposition, requires a thorough understanding of the factors and processes involved in the coastal geomorphological system. Hence, information on winds, waves, tides, currents, geomorphology and the rate of sediment transport along a coast are of paramount importance in understanding the coastal sediment budget and are required for the planning and design of coastal infrastructure.

The aim of this thesis is to develop a coupled framework of three numerical models for the Willoughby Spit-Ocean View Beach in Norfolk (Fig. 1), Virginia, to determine how the shoreline is behaving in response to coastal storms and RSLR. This particular beach is selected because it is a sandy beach that experiences erosion and is of importance to the city in terms of tourism and the protection it provides for upland properties against storms, and because it is located in an area that is experiencing a high rate of RSLR. The sand lost through erosion is replenished after every few years through beach nourishment projects that cost millions of dollars. For example, in 2017, the U.S. Army Corps of Engineers completed a $34.5 million dredging and beach building project that deposited 1.2 million cubic yards of sand which widened the Ocean View beach by about 60 feet. Such projects require long-term shoreline

change data, as well as information on future shoreline erosion rates, to enable better planning and execution.

This study aims to provide a source of information about shoreline response to storm tides, extreme waves and RSLR for the next 50 years at this beach. The model projections on current and expected near-shore coastal hydrodynamic and morphodynamic states related to storm events for the beach could be utilized by the City of Norfolk, by state and federal agencies, and by the general public for decision making, to aid in reducing the risk of extreme events.

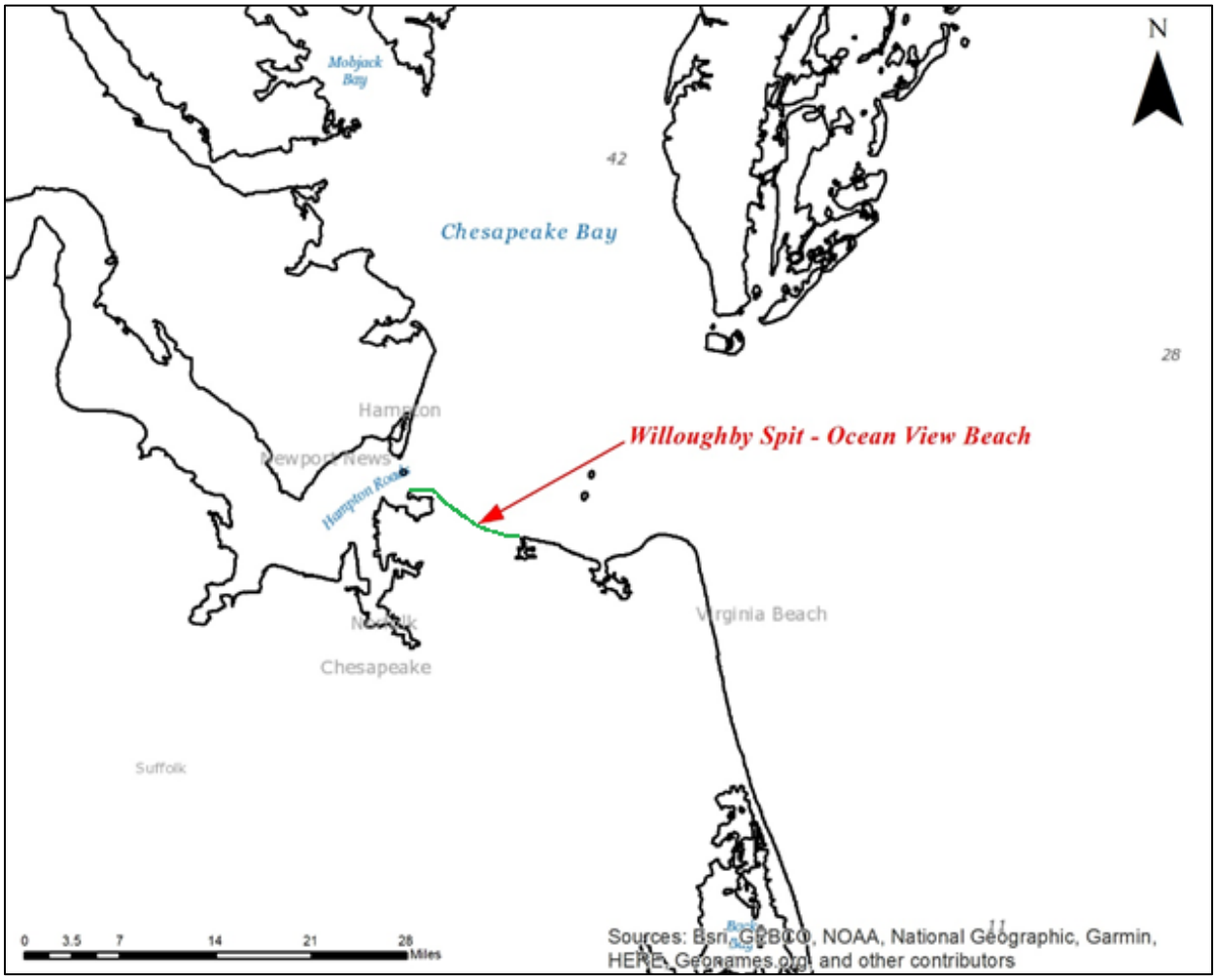

Fig. 1 Location of Willoughby Spit-Ocean View Beach in Norfolk.

CHAPTER 2

LITERATURE REVIEW

Coastal planning and management rely on predictions of hydrodynamics, sediment transport, and morphodynamic change, and numerical models have become important tools to address these needs. Numerical modeling of three-dimensional circulation hydrodynamics began without the influence of waves (Baptista et al., 2005; Banas et al., 2009; Liu et al., 2009). Some of the well-known circulation models are: Delft3D-FLOW (Roelvink and Van Banning, 1995), ADCIRC (Luettich et al., 1992), FVCOM (Chen et al., 2006). However, in recent times, circulation models are being extensively coupled with wave models (e.g. WAVEWATCH III (Tolman, 2009), SWAN (Booij et al., 1999)) to find the influence of waves on flow characteristics, and vice-versa. The ADCIRC+SWAN coupled model has been shown to be effective in capturing the regional surge and wave response of various historical tropical cyclones such as Katrina, Rita (2005), and Gustav (2008) (Rego and Li, 2009; Dietrich et al., 2011). Delft3D FLOW+WAVE coupling has also been tested in various studies (e.g. Hopkins et al., 2016; Mulligan et al., 2008, 2010; Elias et al., 2012).

Numerical models have now evolved to an even better level, and now 2-D and 3-D models of hydrodynamics, waves, sediment transport, and morphology are being coupled. Models such as Delft3D, XBeach (Roelvink et al., 2009), Mike21 (Warren and Bach, 1992), and ROMS (Warner et al., 2010) have been applied, to study sediment transport and geomorphodynamics These coupled systems solve conservation of mass and momentum of fluid and sediment, and seek to resolve nearly all of the important physical processes involved in coastal evolution. These models have become increasingly capable of simulating not only short timescales, from

days to weeks (de Winter et al., 2015), such as beach and dune erosion due to storm events, but they have also achieved realistic simulations on even longer timescales (Luijendijk et al., 2017).

Storm wind fields, tides, and RSLR are the main external forcing factors that are used to force coupled hydrodynamic+wave+sediment transport modeling systems. Tropical and extra-tropical storms are significant hydro-meteorological phenomena that produce coastal flooding and endanger human life. RSLR has the potential to compound the impacts of storm events on the coastal landscape by causing an increase in storm surge (Castrucci and Tahvildari, 2018) and shoreline erosion (Passeri et al., 2015). Increased sea levels allow waves and surges to act at higher levels landward in the beach profile and increase erosion rates (Zhang et al., 2004). As RSLR continues to increase, it will lead to even greater surge heights and morphological changes in the future (FitzGerald et al., 2008). There are a few studies that have explored the role of sea level in storm driven hydrodynamic-morphodynamic interactions. Passeri et al., (2018) examined the morphological response of Dauphin Island, Alabama to storm surge under RSLR. They used the ADCIRC+SWAN model to solve for the flow and wave fields, which was then used in the XBeach model to simulate the morphodynamic change of this barrier island system.

In this study, we investigate the erosion of a sandy beach in detail by using a sequence of coupled Delft3D FLOW-WAVE models which provide boundary conditions at the study area by downscaling the meteorological forcing from basin-wide scale (Chesapeake Bay) to the hotspot domain for the XBeach model in order to simulate coastal erosion. The hydrodynamics and morphodynamics of XBeach, as a modeling tool for coastal change, have been extensively validated against numerous flume experiments (1D) and field case studies (2DH). The model has been successfully applied to sandy beaches at Assateague Island, Maryland (Roelvink et al., 2009), Santa Rosa Island, Florida (McCall et al., 2010), Bay Head, New Jersey (Smallegan et al.,

2016), and Ostend Beach, Belgium (Bolle et al., 2010). Previous studies have also shown that XBeach is capable of simulating storm-driven dune erosion, overwash, inundation, breaching, and seaward sand transport with high skill (Harter and Figlus, 2017; Lindemer et al., 2010; Sherwood et al., 2014). Additionally, XBeach has been successfully coupled, in previous studies, with the Delft3D FLOW+WAVE model. Valchev et al., (2018) used XBeach, along with Delft3D FLOW+WAVE, to validate and implement a coastal forecasting system for Varna Beach in Bulgaria. The triple-coupled interactions and feedbacks between sea level, storms, and morphology provided by this system improve the understanding of longer-term shoreline evolution in the context of storm events.

CHAPTER 3

STUDY AREA

The study area, located at the northern most portion of the city of Norfolk, is a 7.3 mile shoreline stretch extending east from the tip of Willoughby Spit to the inlet at Little Creek (Fig. 2). The shoreline is long and curvilinear, and the beach is mostly sandy, with a system of offshore sand bars, showing that the littoral system is sand rich due to the material coming through the mouth of the bay. Several structural measures, including an array of offshore breakwaters on the eastern Ocean View beach and a series of groins and breakwaters on Willoughby Spit have been constructed to stabilize sediments. These sand bars greatly influence, and are themselves influenced by the wave climate (Hardaway et al., 2005). The location and orientation of the shoreline, which is in the southern Chesapeake Bay and immediately within the mouth of the bay, have exposed it to open bay fetch and oceanic conditions. The large expanse of open water in the Chesapeake Bay to the northwest, north, and northeast allows storm-generated waves to gain strength, making the entire shoreline highly susceptible to coastal storms, such as hurricanes and northeasters. Storm tides, high winds, and wave action associated with these storms impinge on the shoreline, resulting in loss of land (beach erosion) and property damage, and endanger health and safety of the community. In general, the beaches along Willoughby Spit and the western portion of Central Ocean View are mildly erosional, with rates estimated upward of 1.3 feet per year. The eastern portion of Central Ocean View is relatively stable due to the beneficial deposit of the sand migrating from beach nourishment projects to the east. The East Ocean View beaches are the most erosional of the entire study area due to the interruption of the westerly longshore movement of sand by the Little Creek Jetties. Erosion rates up to 5.5 feet per year have been estimated for East Ocean View in the past, and storms continue to have an

impact. However, the construction of the offshore breakwaters in this area has helped to alleviate some of the erosion, resulting in rates that are possibly upward of 2.5 feet per year (USACE, 2014).

Not only does the eroding beach diminish the protective barrier for the bay front, it also adversely affects many of the recreational aspects of the beach, including swimming, fishing, and sunbathing. Over the years, the city of Norfolk has expended significant resources to reduce and/or mitigate the erosion, in order to protect the shoreline. These include a variety of coastal protection structures located along the beach, such as groins, jetties, bulkheads, breakwaters, and revetments. Some of these structures are relatively new, while others are over 70 years old, and their condition varies from good to poor. Numerous beach nourishment projects have also been undertaken during the past fifty years (1953, 1960, 1984, 1989, and 2003) (Elkan et al., 2007). In 2015, the Army Corps of Engineers and the City of Norfolk signed an agreement for construction of a coastal storm damage reduction project. It included placing 1.2 million cubic yards of sand along the shoreline, widening the beach to 60 feet, and creating a slope to 5 feet above mean low water. Completed in mid-May 2017, the project cost around $34.5 million and has an expected life span of 50 years. Over the lifetime of the project, the shoreline is expected to receive 445,100 cubic yards of fill dredged from the Thimble Shoal Auxiliary Channel, every nine years in order to maintain the integrity of the berm.

The Willoughby Spit-Ocean View shoreline has significant societal importance and, hence, its conservation has become an increasing concern. Due its vulnerability and complexity, considerable resources are being spent to protect it, improve its quality and maintain adequate protection of existing and proposed structures, making it an important and interesting study area.

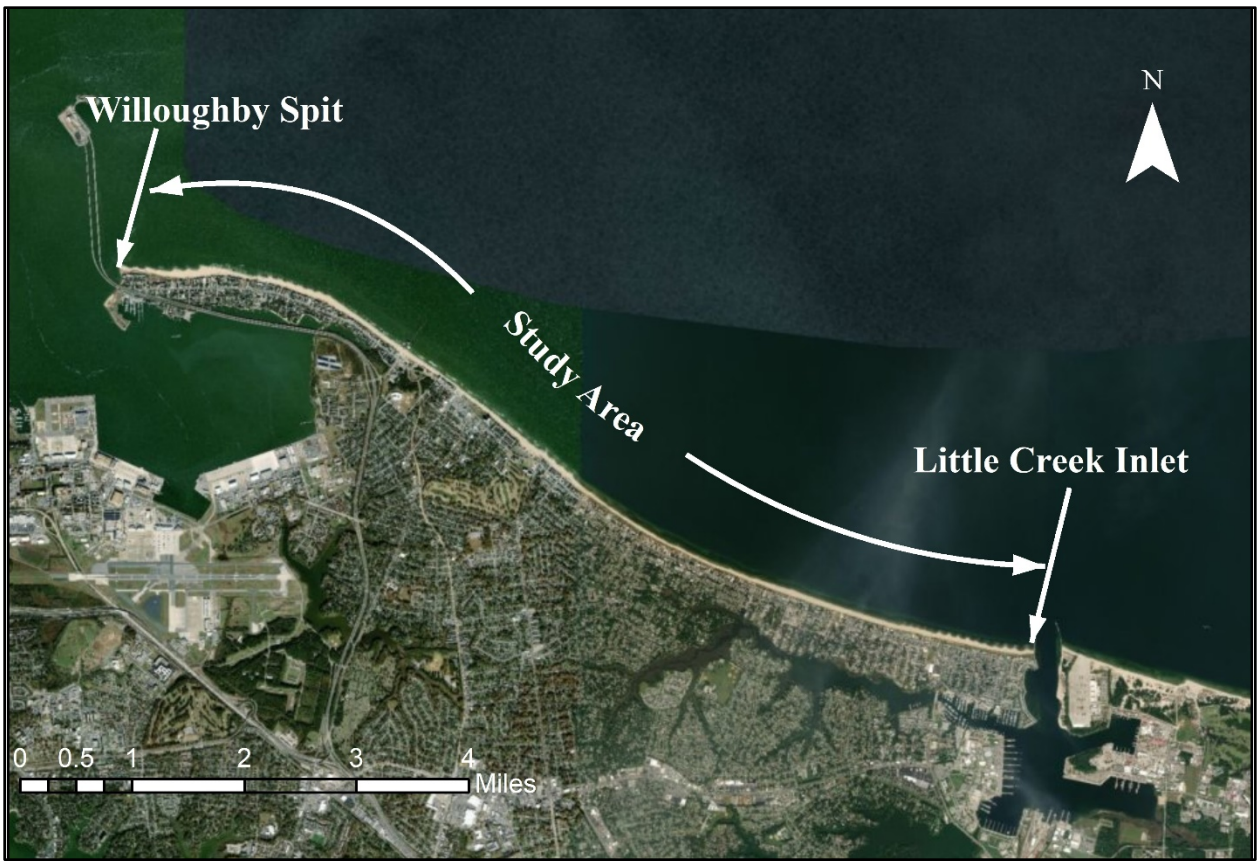

Fig. 2 View of extent of study area.

CHAPTER 4

METHODOLOGY

There is a lack of information regarding the combined effect of RSLR and extreme events on the study area. We use three numerical models to estimate the potential sediment transport, which can inform effective measures to mitigate the coastal erosion problem in the area. The numerical models that solve flow and wave dynamics are based on the Delft3D model. Delft3D is a world-leading 3D modeling suite used to investigate hydrodynamics, sediment transport, morphology, and water quality for fluvial, estuarine, and coastal environments. Two different modules of Delft3D were used, namely Delft3D-FLOW and Delft3D-WAVE. The results obtained after coupling these two modules were given as boundary conditions to the third model, namely XBeach, to calculate the shoreline erosional response. Similar to Delft3D, XBeach is an open source model that has been developed with support from the US Army Corps of Engineers, a consortium of UNESCO-IHE, Deltares, Delft University of Technology and the University of Miami. It is a tool with which the morphological effects due to hurricanes can be simulated and mitigation measures can be evaluated. A brief description of the modeling framework is provided below.

4.1 Modeling Framework

The modeling framework is designed to guarantee a smooth forecasting process; it is a sequence of steps starting with data import, continuing with a few data processing and modeling steps, and resulting in number of predictions for future scenarios. The system is first applied in hindcast mode, through which a past storm event is analyzed and initial states for the models are established through calibration and validation. The hydrodynamic and morphodynamic models

are organized in a chain, so that erosion at the study site can be simulated. The framework works on three levels (Fig. 3). Level one involves the extraction of forcing conditions for Hurricane Irene (2011) (winds and tides) from the global climate and tide models. In level two, the dynamically coupled regional Delft3D-FLOW and Delft3D-WAVE models were set up and forced with datasets obtained in level one to simulate the hydrodynamics for the nearshore study area. For level 3, the nearshore tide and wave boundary conditions obtained from level 2 were used to drive the process-based XBeach model which simulated erosion for a 2D grid and provided a detailed projection of shoreline evolution at regional and temporal scale. Finally, variations in coastal dynamics relative to baseline conditions were evaluated for projected sea level increases for the years 2020, 2030 and 2070, and shoreline response was evaluated.

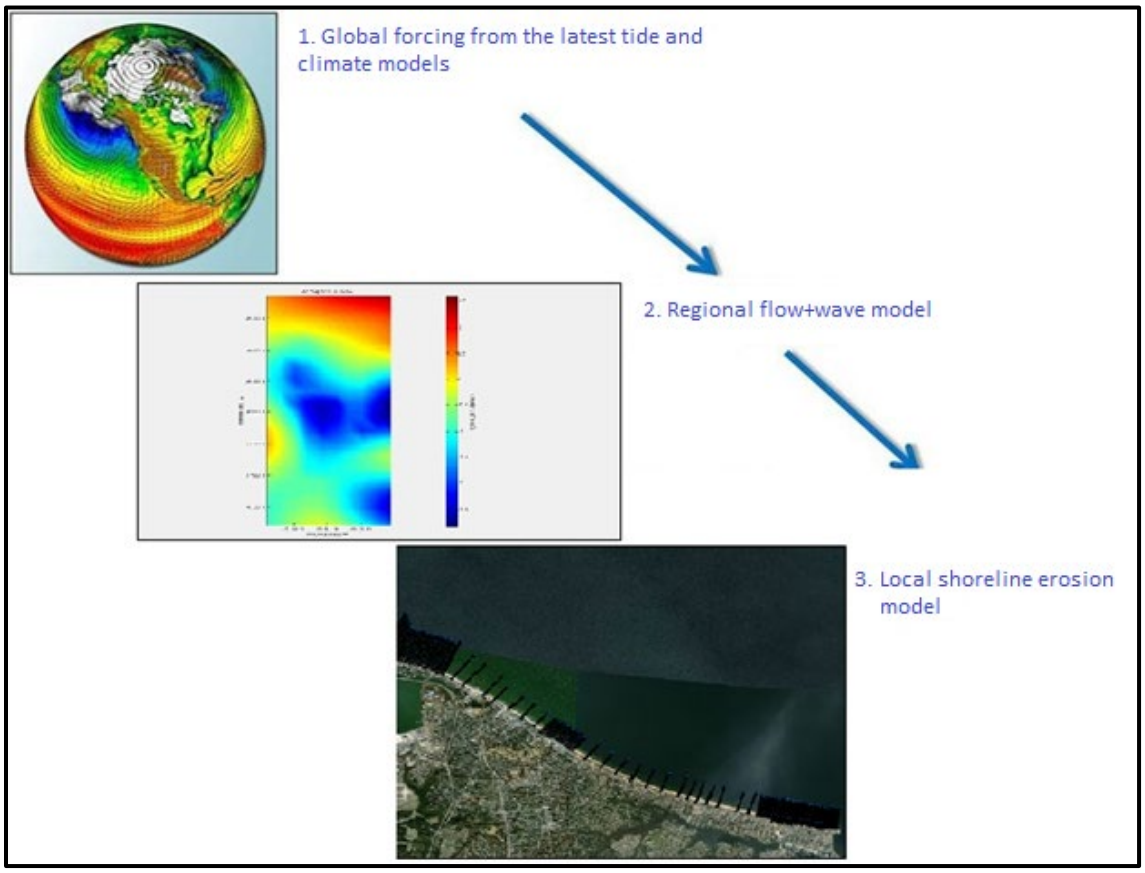

Fig. 3 Schematic view of modeling framework.

4.2 Model Set-up and Governing Equations

4.2.1 Delft3D-FLOW Model

Delft3D-FLOW is an open source, finite difference, multi-dimensional (2D or 3D), hydrodynamic numerical model that has been widely used to investigate unsteady flow processes and transport phenomena resulting from tidal and meteorological forcing (Deltares, 2014). It solves the 3D baroclinic Navier-Stokes equations under shallow-water and Boussinesq assumptions. The equations are as follows:

$$\frac{\partial u}{\partial x} + \frac{\partial v}{\partial y} + \frac{\partial w}{\partial z} = Q, \tag{1}$$

$$\frac{Du}{Dt} = fv - g\frac{\partial \zeta}{\partial x} - \frac{g}{\rho_o}\int_{z'=z}^{z'=\zeta} \frac{\partial \rho}{\partial x} dz' + \nu_h\left(\frac{\partial^2 u}{\partial x^2} + \frac{\partial^2 u}{\partial y^2}\right) + \nu_v\left(\frac{\partial^2 u}{\partial z^2}\right), \tag{2}$$

$$\frac{Dv}{Dt} = -fu - g\frac{\partial \zeta}{\partial y} - \frac{g}{\rho_o}\int_{z'=z}^{z'=\zeta} \frac{\partial \rho}{\partial y} dz' + \nu_h\left(\frac{\partial^2 v}{\partial x^2} + \frac{\partial^2 v}{\partial y^2}\right) + \nu_v\left(\frac{\partial^2 v}{\partial z^2}\right), \tag{3}$$

$$\frac{\partial p}{\partial z} = -\rho g, \tag{4}$$

$$\frac{Dc}{Dt} = D_h\left(\frac{\partial^2 c}{\partial x^2} + \frac{\partial^2 c}{\partial y^2}\right) + D_v\left(\frac{\partial^2 c}{\partial z^2}\right) - \lambda_d c + R_s. \tag{5}$$

Eq. (1) represents conservation of mass under the assumption of incompressibility; Eq. (2) represents the conservation of momentum in the *x*- and *y*-directions; Eq. (3) expresses the conservation of momentum in the vertical direction which, under the shallow-water assumption, simplifies to the hydrostatic pressure distribution, which means that the vertical accelerations are assumed to be negligible, compared to the gravitational acceleration; Eq. (4) governs pressure distribution, and finally, Eq. (5) is the transport equation, which is solved in the present study for both salinity and temperature. In these equations, *x*, *y* and *z* represent the east, north and vertical

axes, respectively and u, v and w are the velocity components in the aforementioned directions; ζ is the free surface elevation above the datum; Q represents the intensity of mass sources per unit area; f is the Coriolis parameter; g is the gravitational acceleration; υ_h and υ_v are the horizontal and vertical eddy-viscosity coefficients, respectively; and ρ and ρ_o are the density and the reference density of sea water, respectively. Finally, in the transport equation, c stands for salinity or temperature; D_h and D_v are the horizontal and vertical eddy-diffusivity coefficients, respectively; λ_d represents the first order decay process; and R_s is the source term per unit area.

4.2.2 Delft3D-WAVE Model

Delft3D-WAVE is a derivative of the third generation SWAN (Simulating WAves Nearshore) model (Booij et al., 1999; Ris et al., 1999) and is used to simulate random, short-crested wind-generated surface waves in coastal waters with deep, intermediate, and shallow water and ambient currents. SWAN is the successor of the second generation HISWA model and is based on the discrete action balance equation. It accounts for (refractive) propagation due to current and depth and represents the processes of wave generation by wind, dissipation due to whitecapping, bottom friction, depth-induced wave breaking, and non-linear wave-wave interactions (both quadruplets and triads) (Deltares, 2014). SWAN considers the action density spectrum $N(\sigma, \theta)$ rather than the energy density spectrum $E(\sigma, \theta)$, since the former is conserved in the presence of currents (Whitham, 1974). The evolution of wave spectrum is described by the spectral action balance equation (Hasselmann et al., 1973).

$$\frac{\partial}{\partial t}N + \frac{\partial}{\partial x}c_x N + \frac{\partial}{\partial y}c_y N + \frac{\partial}{\partial \sigma}c_\sigma N + \frac{\partial}{\partial \theta}c_\theta N = \frac{S}{\sigma} \tag{6}$$

The right hand side of the equation represents the source term S (= $S(\sigma, \theta)$) in terms of energy density considering the effects of generation, dissipation and non-linear wave-wave interactions. The first term on the left-hand side of the equation represents the local rate of change of action density in time, while the second and third terms represent the propagation of action in geographical space, where c_x and c_y are propagation velocities in x- and y-space, respectively. The fourth term quantifies shifting of the relative frequency because of variations in depths and currents, where c_σ is the propagation velocity in σ-space. The fifth term takes into account the depth-induced and current induced refraction, where c_θ is the propagation velocity in θ-space. The expressions for these propagation speeds are taken from linear wave theory (Whitham, 1974; Mei, 1983; Dingemans, 1997).

4.2.3 Coupling of Flow and Wave Models

Storm wave events play an important role in circulation along beaches (Bowen and Inman, 1969; Feddersen and Guza, 2003) hence, the hydrodynamic Delft3D-FLOW model was coupled with wind-wave SWAN (Delft3D-WAVE) model, in order to simulate the nearshore hydrodynamics.

The FLOW part of the coupled model was implemented on two, two-way coupled domains of different resolutions through the Domain Decomposition (DD) approach, a technique in which a model is divided into several smaller model domains and the computations are then carried out concurrently on these domains. The communication between the domains takes place along internal boundaries or so-called DD-boundaries. The DD approach allows for local grid refinement, both in horizontal and vertical directions for adequately simulating the physical processes. Since our model is depth-averaged, only horizontal grid refinement was performed,

meaning that one domain has a smaller mesh size (fine grid: Grid 2) than the other domain (coarse grid: Grid 1). DD method is an accurate, computationally efficient, and flexible tool for simulating complex physical processes.

In the present study, the domain decomposed flow was simulated at a time step of 0.05 min to satisfy the Courant–Freidrichs–Lewy condition, which is governed by the grid size of the higher resolution grid. This also reduces numerical error and ensures the stability of the model. The resolution of the two domains was selected to resolve the necessary nearshore processes (e.g. surfzone processes and tidal propagation).

Delft3D-WAVE, on the other hand, supports one-way nesting of computational grids in wave computation. The idea behind this is to have a coarse grid for a large area and one or more finer grids for smaller areas. Computation for the coarse grid is executed first, and the finer grid computations use these results to determine their boundary conditions. In this module, the same two grids which were used in the FLOW module are nested one-way to propagate waves from offshore into the nearshore.

Delft3D-FLOW and Delft3D-WAVE models were dynamically coupled (i.e., two-way wave-current interaction) for Hurricane Irene surge simulation, where information was passed between the two models at 60 min intervals to account for the nonstationary nature of coastal storms (Xie et al., 2008). By this, the effect of currents and water levels on waves, including wave setup and the effect of waves on currents and water levels, can be accounted for. Wave effects, including wave-driven radiation stresses and enhanced bed shear stresses, are integrated in the flow simulation. The wave forces computed in Delft3D-WAVE enhance the energy dissipation at the bed boundary layer in the storm surge model and generate a net mass flux, affecting the current. These effects are accounted for by passing the radiation stress gradient

determined from the computed wave parameters from Delft3D-WAVE to Delft3D-FLOW model. The water levels and currents computed by the Delft3D-FLOW model are then passed back to the Delft3D-WAVE model for more accurate wave estimates (Deltares, 2014). This constant exchange of information is achieved through a communication file which stores information from one module and passes it to the other. The coupling process makes the inputs for Delft3D-FLOW consistent with the ones for SWAN. The two modules share the same grid, topography, bathymetry, and wind and pressure data. The coupled model was run on a cluster that has 2 Intel(R) Xeon(R) Gold 6148 CPUs, with a processing speed of 2.4GHz for each node. During the model run, the two modules of the coupled system used different number of processing cores, based on their specific limitations. Delft3D-FLOW only used two cores, one each for the two domains, as domain decomposition does not support parallel computation, whereas Delft3D-WAVE used 40 cores. The computational time for this coupled system was around 6-8 days for one run.

4.2.3.1 Grid Generation

For any numerical model, grid schematization is a tradeoff between computational time and modeled processes. Grid resolution and time step should be sufficient to capture the phenomena of interest, but they should still allow efficient and accurate computations. Two equidistant, orthogonal, structured rectilinear grids were set up at different resolutions to accurately capture the dominant processes at the study area, including tides, waves, wind driven flows, currents and their interactions. For the flow model, two-way coupling of the grids was achieved through the DD technique, which allowed the two grids to be of different resolutions, have no overlap, and be run on a separate processing core, in order to improve computational efficiency (Hummel and

de Goede, 2000). Fig. 6 shows the two grids separated by a DD boundary in DD mode. The same grids were nested one-way in the SWAN model for wave simulation. The coarser grid (Grid 1 shown in Fig. 4) covers almost the entire Chesapeake Bay and has a resolution of 125 x 200 m^2. It should be noted that, in order to produce accurate results, meteorological forcing and boundary conditions need to be provided to the model at high resolution. The benefit of having such a large domain is the simplicity of boundary conditions, since the open boundaries are primarily located in the deep ocean, reducing the boundary effects on the area of interest. The finer grid (Grid 2 shown in Fig. 5) has a higher resolution of 10 x 10 m^2 and has its offshore boundary a few kilometers away from the shoreline so that there is no breaking near its boundary and unrealistic strong wave-driven currents are avoided. Having a finer grid resolution aids in capturing the propagation and evolution of the dominant processes nearshore where the bathymetry is complex (Hagen et al., 2001). Both grids are defined in the Cartesian convention.

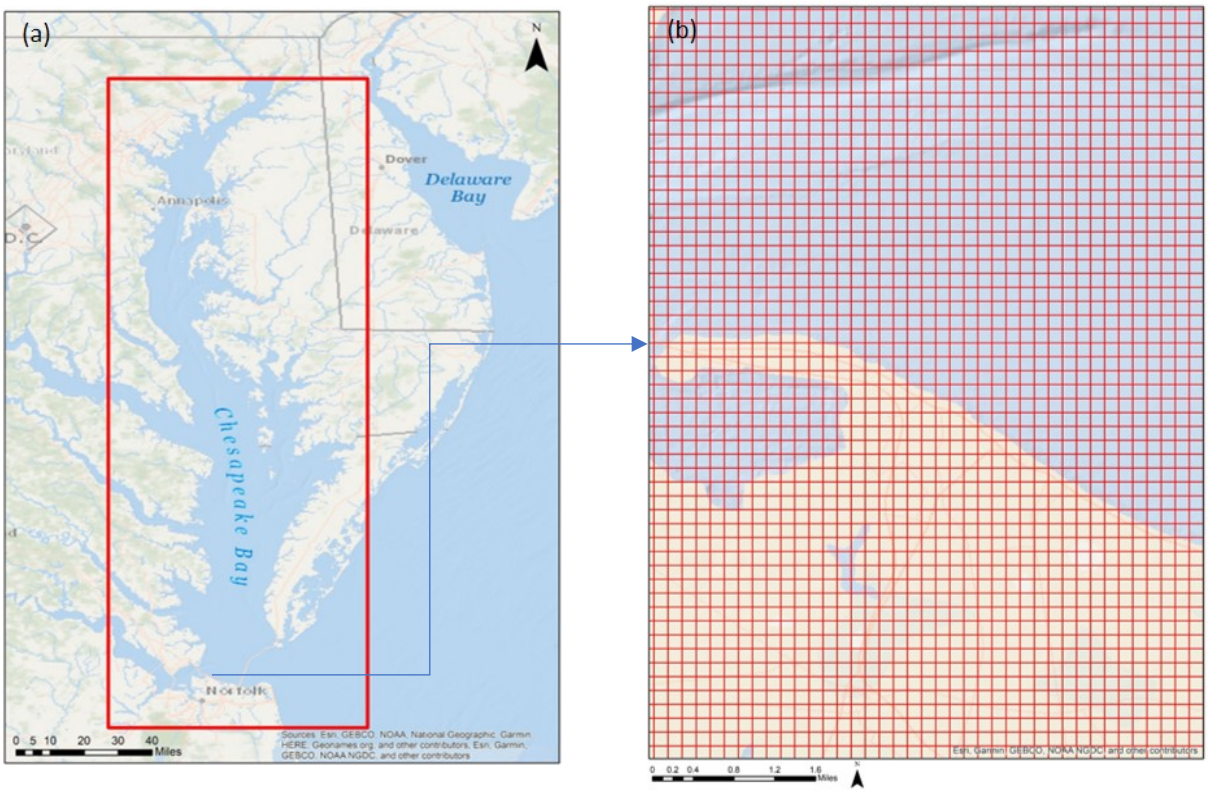

Fig. 4(a) Boundaries of Grid 1 domain and (b) Grid 1 projected on a segment of the study area.

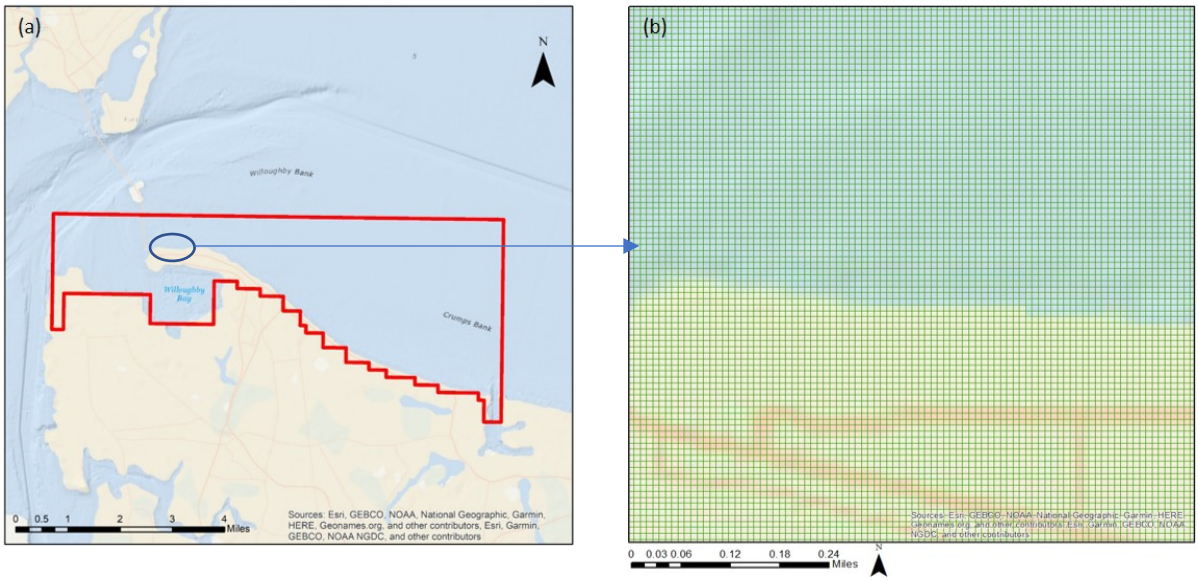

Fig. 5(a) Boundaries of Grid 2 domain and (b) Grid 2 projected on a segment of the study area.

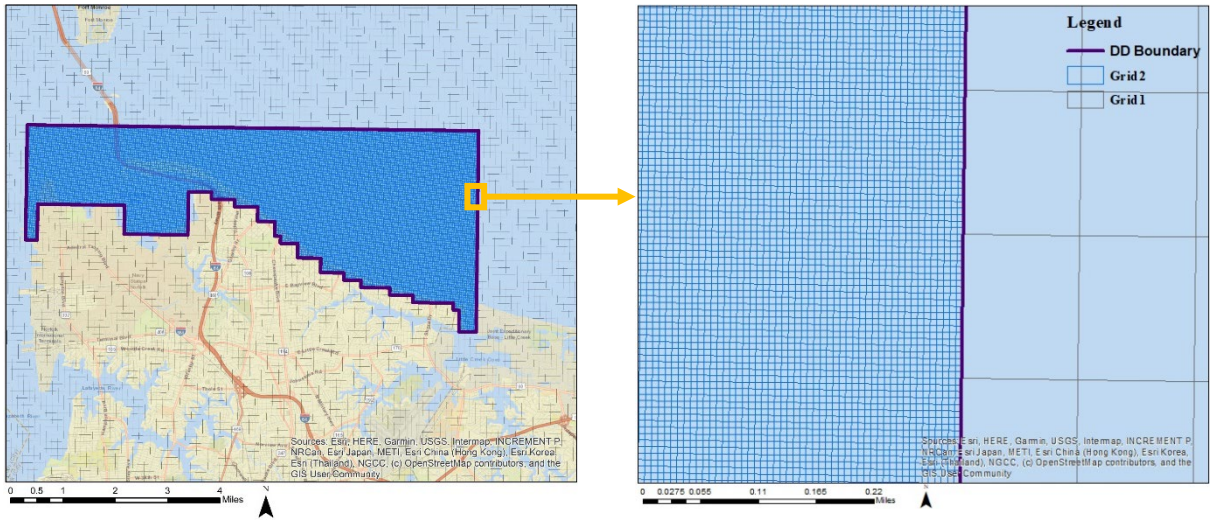

Fig. 6 View of Grid 1 and Grid 2 set-up in domain decomposition mode.

4.2.3.2 Boundary Conditions

To simulate Hurricane Irene-like conditions, the coupled FLOW+WAVE model required tides, winds, atmospheric pressure as forcing conditions, and bathymetric and topographic data.

The governing equations were then solved over computational grids. In this section, we discuss the required boundary conditions.

4.2.3.2.1 Tides and Wind Forcing

TPXO global tide model (Egbert and Erofeeva, 2002) was used to extract the tidal elevation and phase of the primary nine tidal constituents (M2, S2, N2, K2, K1, O1, P1, Q1 and M4) used for forcing the coupled FLOW+WAVE model. The astronomical tidal conditions were provided at the open boundary of the coarser grid (Grid 1) at a resolution of 1/30º.

Flow and wave models are highly sensitive to input wind fields and atmospheric pressure; hence high-resolution and high-accuracy winds are required to reproduce the storm surge and wave conditions (Janssen, 1989; Feng et al., 2006). Thus, the coupled model was forced, for Hurricane Irene scenario, with high resolution CFSv2 (Saha et al., 2014) u and v wind components obtained from the NCEP (National Centers for Environmental Prediction) with a time step of 1 h and a resolution of 0.2º. CFSv2 also provided the atmospheric pressure time-series at a similar resolution for the simulation. The time and space varying wind components (east-west and south-north) and atmospheric pressure were specified on separate equidistant rectilinear grids covering the entire Chesapeake Bay. Fig. 7(a) shows the contour plot of wind forcing at a particular time step during Hurricane Irene on an equidistant grid. Delft3D then estimated the wind and pressure forces acting on water level and waves through the interpolation between the meteorological and hydrodynamic domains. The model performance was validated against the 2011 storm surge level and wave parameters, and was further used to simulate flow-wave conditions due to Irene-like storms under future sea level scenarios.

4.2.3.2.2 Topographic and Bathymetric Data

Bathymetry and topography play a crucial role in determining the accuracy of the model (Elias et al., 2012, Sebastian et al., 2014). We used the freely available data from NOAA's Coastal Relief Model having a horizontal resolution of 90 m for Grid 1, whereas for Grid 2, NOAA's 1/3 Arc second Virginia Beach Digital Elevation Model (horizontal resolution 10 m – 90 m) was used. Fig. 7(b) shows a contour plot of topography/bathymetry data in the study area. Samples (x, y, z) for our model grids were extracted from the NetCDF DEM file using MATLAB. Triangular interpolation and internal diffusion methods in the Delft3D QUICKIN module were utilized to interpolate the datasets onto model grid points.

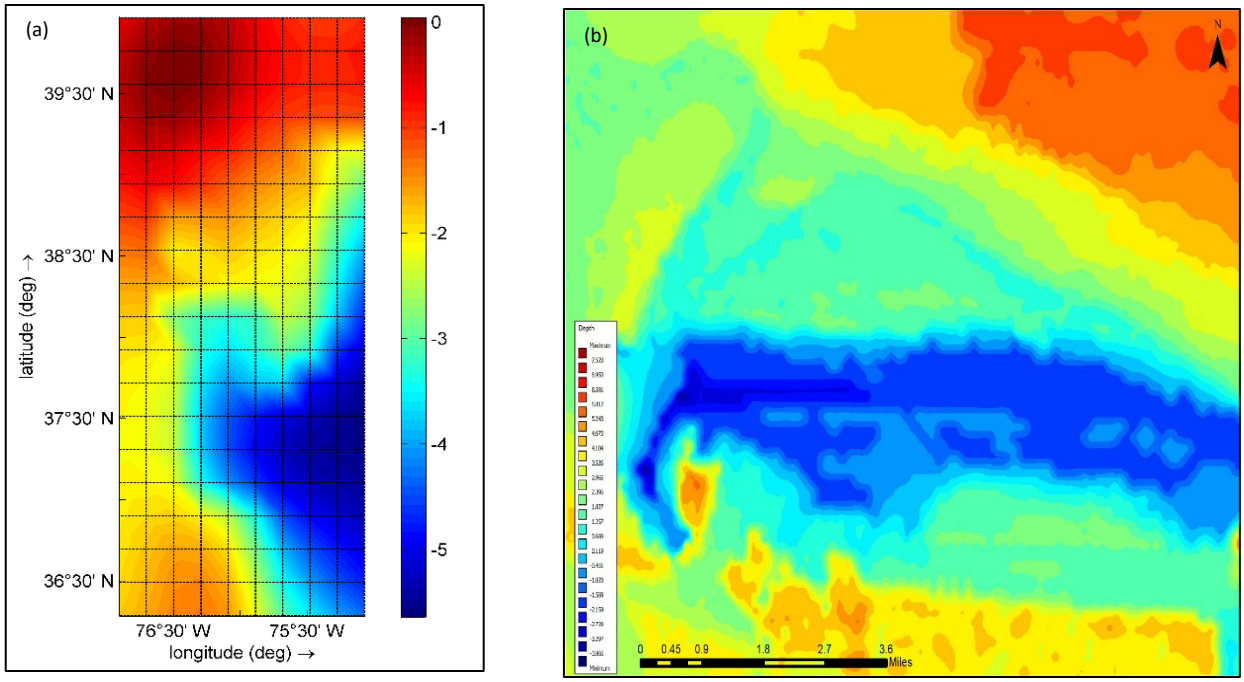

Fig. 7 View of boundary conditions (a) contour plot of equidistant wind forcing in m/s and (b) contour plot of topographic/bathymetric data.

4.2.4 XBeach Model

The XBeach model by (Roelvink et al., 2009) is a depth- averaged, numerical model that solves the coupled 2DH equations for long wave propagation, short wave energy, flow, sediment transport, and bottom changes of the nearshore area, beaches, dunes and backbarrier during time-varying storm conditions. The morphodynamic processes include bed load and suspended sediment transport, dune face avalanching, bed update and breaching. The effects of vegetation and of hard structures have also been considered. XBeach offers two sediment transport formulations, namely Soulsby-Van Rijn and Van Thiel-Van Rijn, that solve the 2D horizontal advection-diffusion equation (Galappatti and Vreugdenhil, 1985) and produce total transport vectors.

$$\frac{\partial hC}{\partial t} + \frac{\partial hCu^E}{\partial x} + \frac{\partial hCv^E}{\partial y} + \frac{\partial}{\partial x}\left[D_h h \frac{\partial C}{\partial x}\right] + \frac{\partial}{\partial y}\left[D_h h \frac{\partial C}{\partial y}\right] = \frac{hC_{eq} - hC}{T_s} \quad (7)$$

In the above equation, C is the depth-averaged sediment concentration varying on the wave-group time scale and D_h represents the sediment diffusion coefficient. T_s is the adaption time and denotes the entrainment of sediment, which can be approximated using local water depth $\underline{h}$ and sediment fall velocity w_s.

To observe the morphodynamic response of Willoughby Spit-Ocean View Beach to the combined impacts of storm surge, waves, and RSLR, a dynamic modeling approach was implemented. Sediment transport and bed level change were simulated using XBeach. The model was implemented in the 'surfbeat' mode, which includes run-up and run-down of long waves (swash) and a morphological acceleration factor of 10 (Ranasinghe et al., 2011). The hard structures, such as breakwaters, groins etc., located within the study area were presented as a

non-erodible layer. Beach sediments were defined as a single sediment fraction with D_{50} of 0.5 mm (USACE, 2014).

4.2.4.1 Grid Generation

A 2D grid was set up to calculate the shoreline evolution due to storm tides and sea level rise. This grid has its seaward boundary (6 m depth) at approximately 500 m away from the region of interest and covers the entire Willoughby Spit- Ocean View 7.3 km shoreline. It is curvilinear, non-equidistant grid with cross-shore (*dx*) and alongshore(*dy*) grid size ranging from 1-3 m (Fig. 8). Such a high resolution was chosen in order to accurately capture the exact shape of the dune face. The grid is defined in the Cartesian convention.

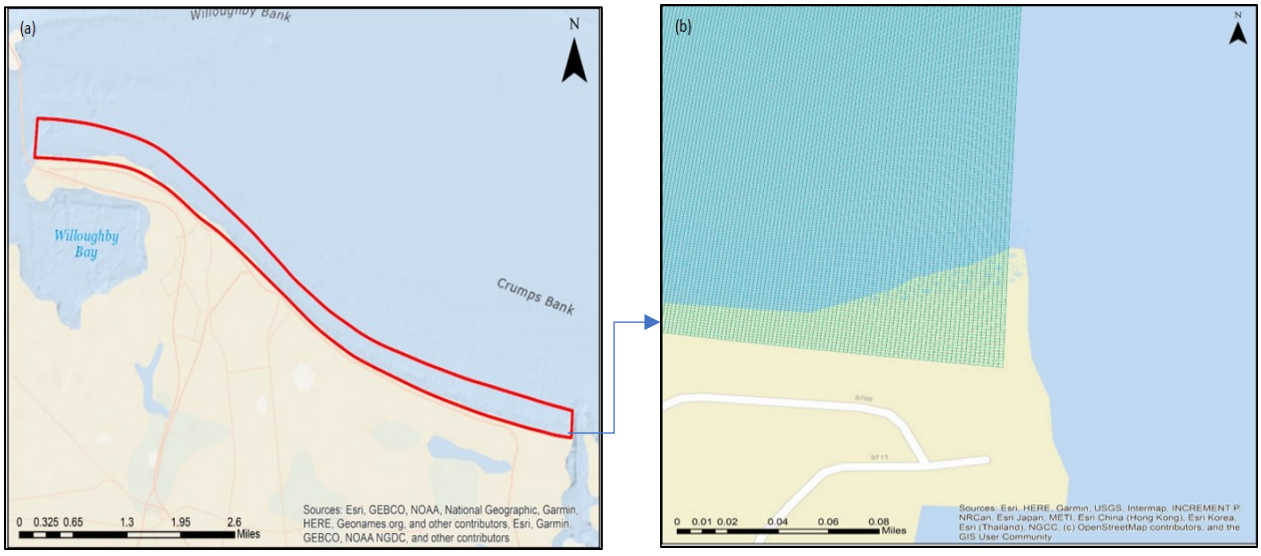

Fig. 8(a) Boundaries of XBeach domain and (b) Computational grid projected on a segment of the study area.

4.2.4.2 Boundary Conditions

The specific geography and hydrodynamics of the study area required XBeach to integrate tide, surge, wave characteristics, and setup in the boundary conditions. Water level, wave

spectra, nearshore bathymetry and topography were used to force the model. Periodic topographic and bathymetric beach surveys are carried out by Moffat and Nichol (contracted by the city of Norfolk) and the data is available for the year 2011. Measurements for pre-storm bathymetry were not available; thus, data surveyed for the month of April 2011, which was the latest survey prior to the storm that happened in August 2011, was used as topographic and bathymetric model input (Fig. 9). Water level time-series were provided at the four corners of the XBeach grid, whereas wave parameters were provided at the offshore boundary in the form of 2D spectra files obtained from the coupled flow-wave simulation.

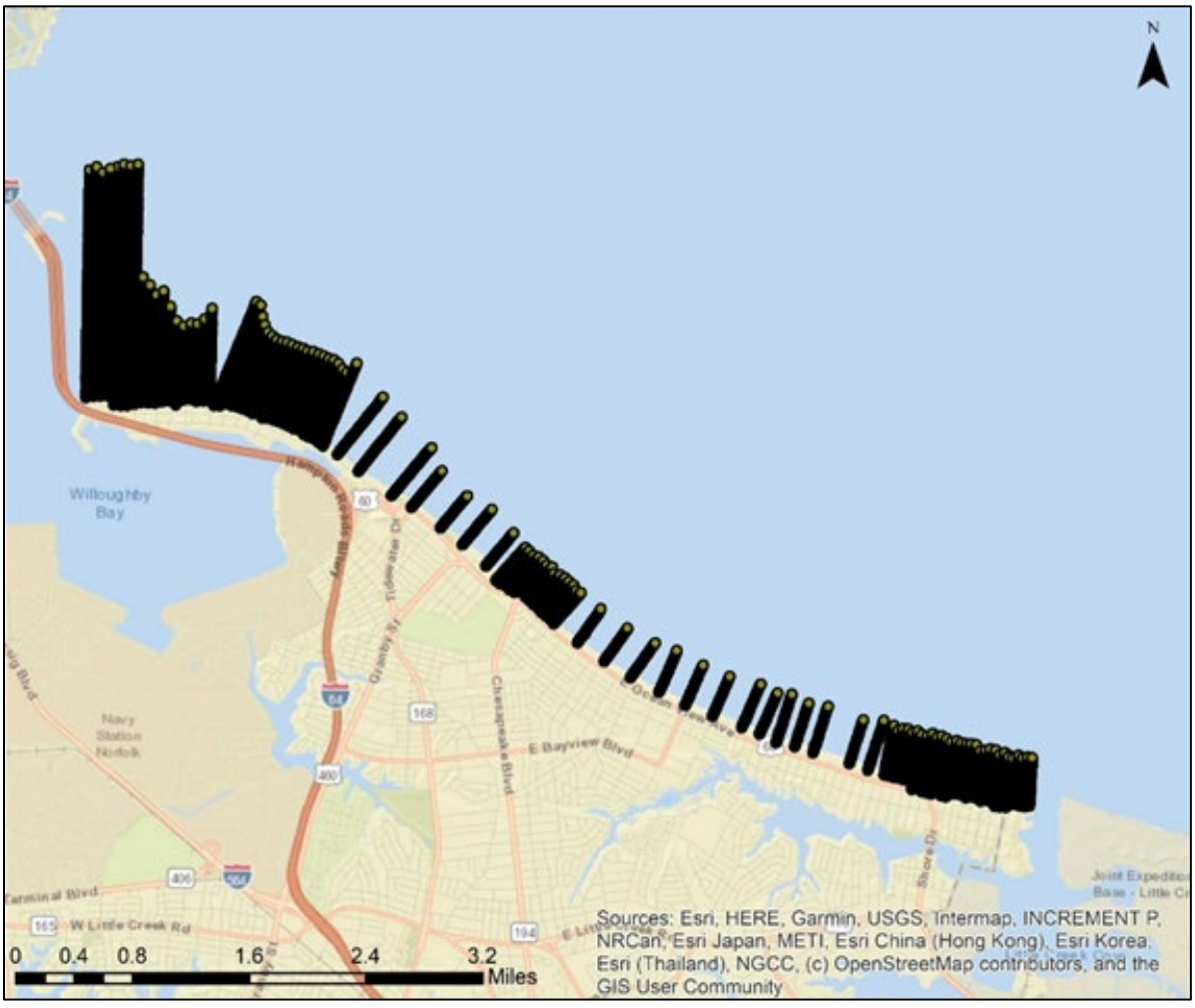

Fig. 9 Plan view of topographic/bathymetric transects survey.

4.3 Relative Sea Level Rise

RSLR can aggravate the impacts of extreme storm events on the coastal landscape. To incorporate RSLR into our estimations, the initial water level was offset by the amount of RSLR in Delft3D-FLOW; this dynamic approach captures the nonlinearities in the governing equations, and hence, provides more accurate assessments than the static or "bathtub" approach, in which present-day water levels are directly elevated by the amount of RSLR (Hagen and Bacopoulos, 2012). Many studies have shown that storm surge under RSLR increases nonlinearly (Atkinson et al., 2013; Bilskie et al., 2014; Mousavi et al., 2011; Smith et al., 2010; Yin et al., 2017, Castrucci and Tahvildari, 2018), and the offset method of increasing the water level to the desired RSLR values at the model boundaries used in this study aims to capture that non-linearity. Three RSLR scenarios, i.e., Medium (M), Intermediate-High (IH), and High(H), each for 2020, 2030 and 2070 from NOAA's 2017 technical report (Sweet et al., 2017) were considered. Table (1) summarizes the estimates for 2020, 2030 and 2070.

Table 1. RSLR scenarios used in FLOW +WAVE simulations. The values are based on NOAA Technical Report NOS CO-OPS 083 (Sweet et al., 2017).

Relative Sea Level Rise (m)	2020	2030	2070
Medium (M)	0.09	0.20	0.75
Intermediate-High (IH)	0.14	0.28	1.09
High (H)	0.18	0.36	1.49

CHAPTER 5

RESULTS

5. 1 Calibration and Validation

5.1.1 Flow-Wave Coupled Model

Delft3D-FLOW and Delft3D-WAVE allow the user to have considerable control of the hydrodynamic processes. Both models are highly parameterized, which allowed us to vary different physical settings, such as water density, air density, gravitational constant, horizontal eddy viscosity, bottom roughness and wind drag coefficients, as well as numerical settings including numerical convergence criteria, numerical solution technique, and wetting drying thresholds for calibration purposes. These parameters were calibrated for the Hurricane Irene coupled hydrodynamic+wave simulation and were then kept constant for simulations with future RSLR. The values of the parameters after calibration are shown in Table (2).

Table 2. Final values of calibration parameters.

Sea water density	1025 kg/m^3
Air density	1.15 kg/m3
Bottom roughness represented by the Manning coefficient	0.015
Horizontal eddy viscosity	1 m^2/s
Threshold depth for wetting and drying	0.1 m
Bottom Friction type	Jonswap
Bottom Friction coefficient	0.067 m^2s^{-3}

Validation was done by direct comparison between model output and measurements gathered during the same period and calculation of their overall root-mean square errors and correlation coefficient. The output parameters of interest were water level, significant wave height (H_s), peak wave period (T_p) and mean wave direction (D_m), as well as 2D wave spectra. Due to the unavailability of peak wave period measurements, comparison was done for mean wave period measurements and mean wave period model output. The aim of validation was to examine the quality of boundary conditions, at both grids, generated by Delft3D FLOW+WAVE model, which eventually fed the erosion model. Validation was carried out at observation points in Grids 1 and 2. Table (3) show the sources of data that were used for model validation at Levels 1 and 2.

Table 3. Observation points for Grid 1 and Grid 2.

	Type of Instrument	Source	Location
Grid 1	Tide Gauge	NOAA	Chesapeake Bay Bridge Tunnel (CBBT)
	Wave Gauge	CBIBS	Stingray Point
Grid 2	Tide Gauge	NOAA	Sewell's Point
	Acoustic Wave and Current Gauge (AWAC)	City of Norfolk	Lat – 36.963^o Lon –76.229^o

We used the data at the Chesapeake Bay Bridge and Tunnel (CBBT) tide gauge and the wave data from the buoy at Stingray Point operated by the Chesapeake Bay Interpretive Buoy System (CBIBS) (shown in Fig. 10) for validating Model 1. Fig. 11(a) and (b) show excellent agreement between model prediction for water level and significant wave height with measurements at these sensors during Hurricane Irene. Fig. 11(c) and (d) shows a good

agreement between model results for mean wave period and direction with measurements at the wave buoy. It is noted that relatively high uncertainty in wave direction causes some deviation in model results from measurements. Table (4) summarizes the error statistics for Grid 1 model parameters. As seen, the Root Mean Square Error (RMSE) and r^2 are satisfactory for all of the parameters, except for wave direction.

For Model 2 validation, we used the water level data at the Sewell's Point tide gauge and the wave data from the Acoustic Wave and Current Gauge (AWAC) deployed by the city of Norfolk approximately one mile off the Willoughby Spit-Ocean View Beach and five miles west of Little Creek Naval Base (shown in Fig. 10). Fig. 12(a) and (b) show excellent agreement between model prediction for water level and significant wave height with measurements at these sensors during Hurricane Irene. Fig. 12(c) shows a good agreement between model results for mean wave period; however, the comparison of mean wave direction with wave buoy data (Fig. 12(d)) shows some phase shift. The results are still acceptable, because during the peak storm conditions (27-28 August 2011), the model compares well and, hence, could be used for the XBeach simulation. Table (5) summarizes the error statistics for Grid 2 model parameters. As seen, the Root Mean Square Error (RMSE) and r^2 are satisfactory for all of the parameters, except for wave direction.

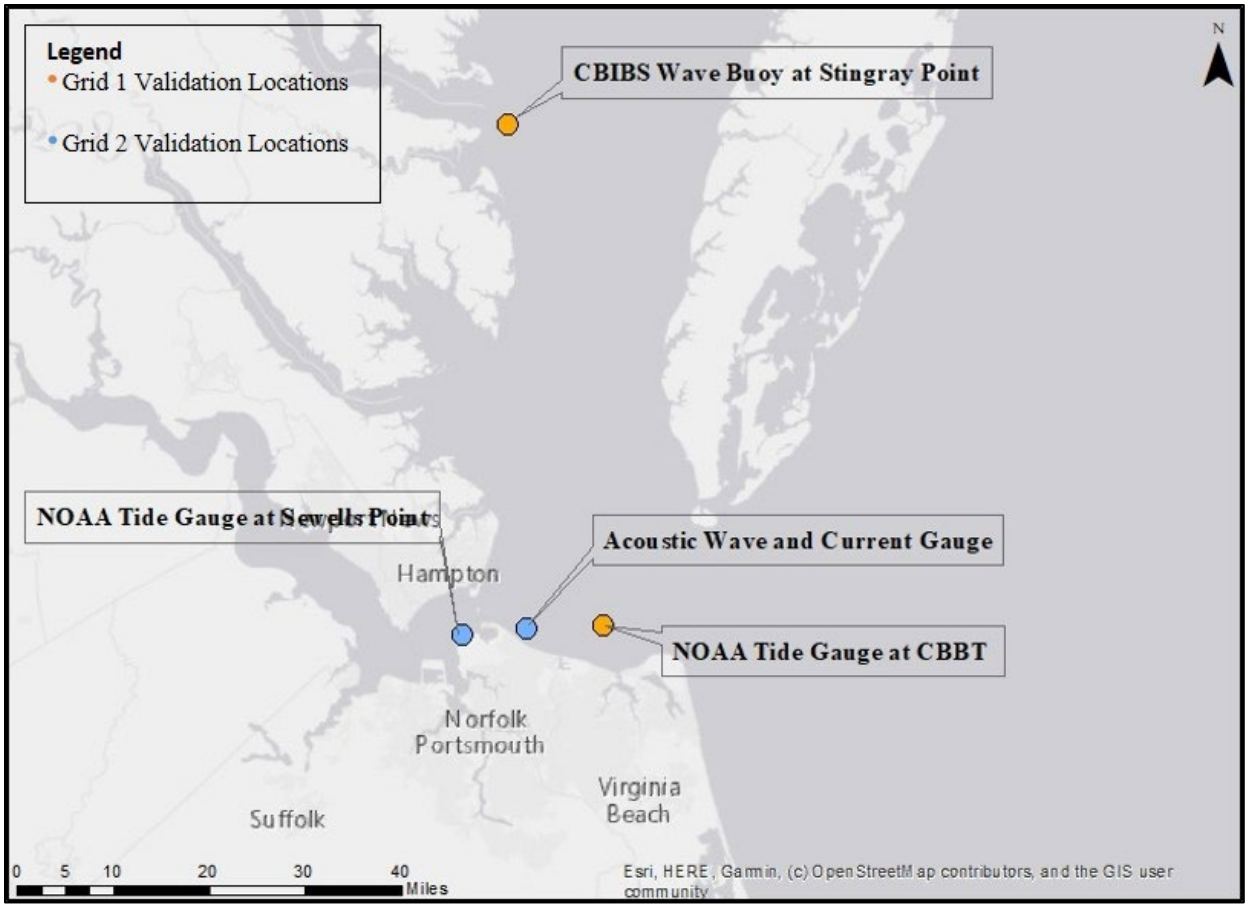

Fig. 10 Locations of tide and wave gauges used for model calibration and validation.

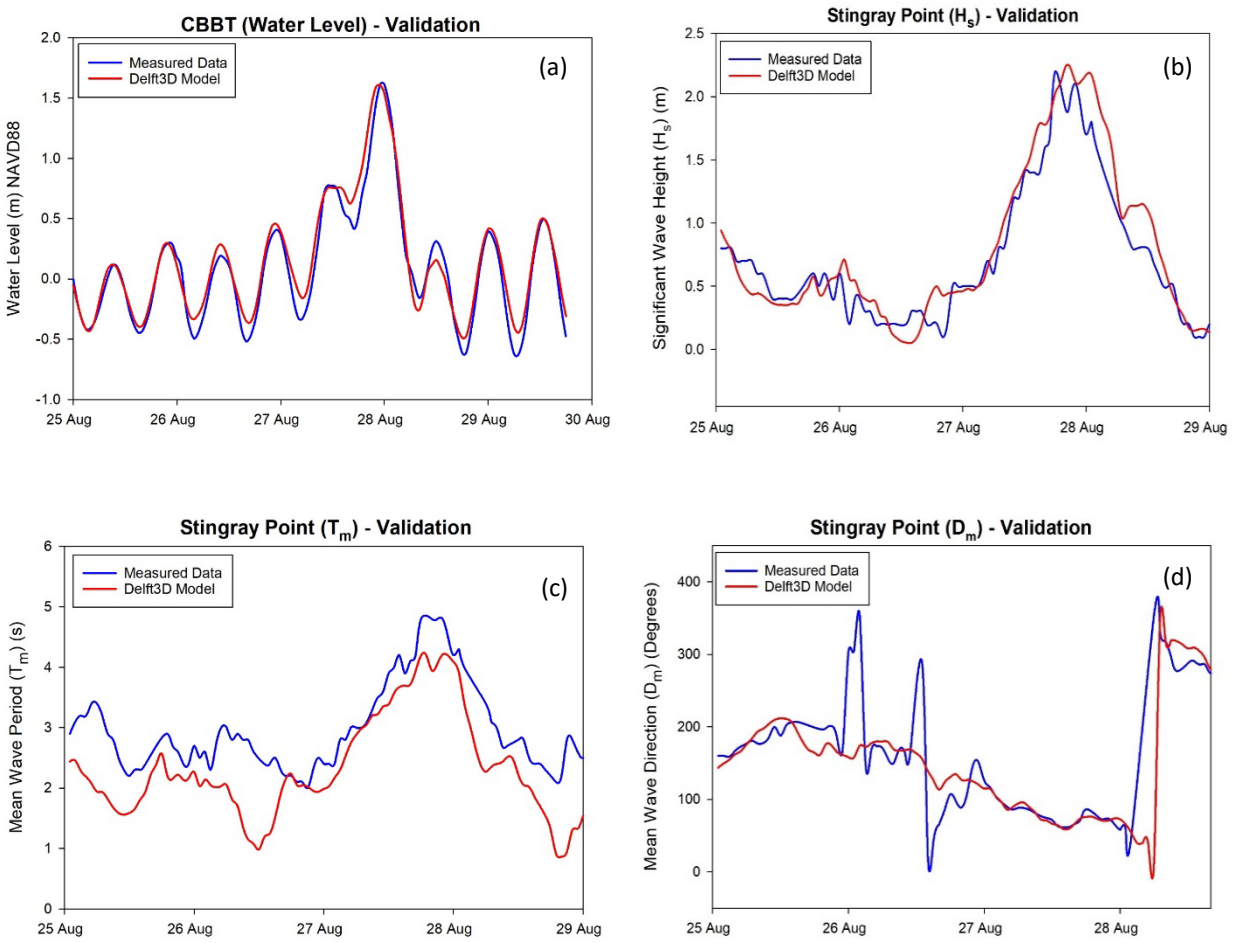

Fig. 11 Model validation for Grid 1 observation points with in-situ measured data(a) Water level comparison (b) Significant wave height comparison (c) Mean wave period comparison and (d) Mean wave direction comparison.

Table 4. Error statistics of Grid 1 model parameters for the selected locations.

Grid 1 Validation Locations	Parameter	RMSE	r^2
CBBT	Water Level	0.115 m	0.958
Stingray Point	Significant Wave Height	0.182 m	0.928
	Mean Wave Period	0.771 s	0.735
	Mean Wave Direction	55.874°	0.572

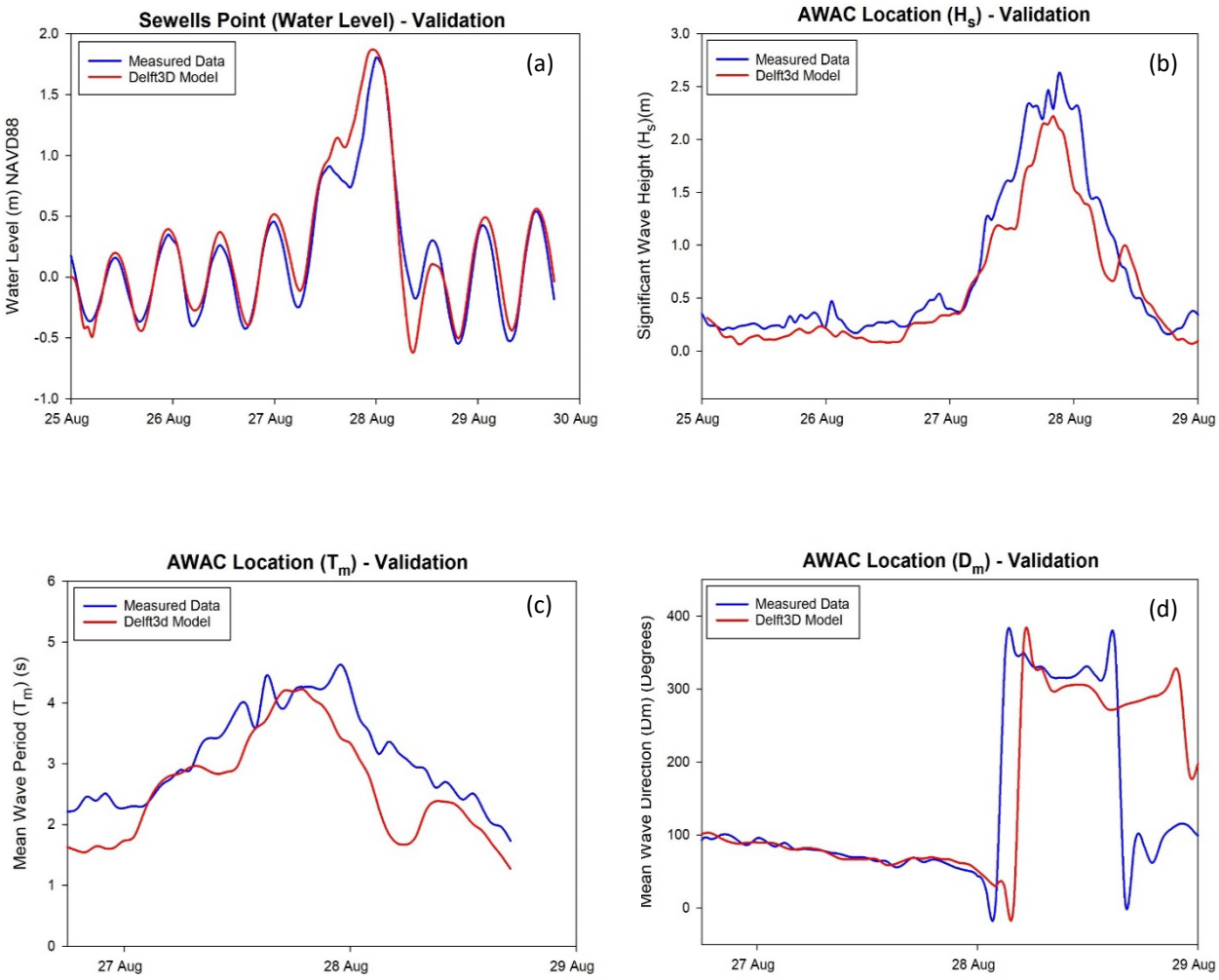

Fig. 12 Model validation for Grid 2 observation points with in-situ measured data (a) Water level comparison (b) Significant wave height comparison (c) Mean wave period comparison and (d) Mean wave direction comparison.

Table 5. Error statistics of Grid 2 model parameters for the selected locations.

Grid 2 Validation Locations	Parameter	RMSE	r^2
Sewell's Point	Water Level	0.165 m	0.932
AWAC Location	Significant Wave Height	0.264 m	0.941
	Mean Wave Period	0.666 s	0.763
	Mean Wave Direction	101.986°	0.342

5.1.2 XBeach Model

The goal of the calibration study was to find the values for model parameters that would give an optimal computational response in order to reach a satisfactory fit to the measured cross-shore profile based on statistical comparison. The default model settings were not an adequate match to the observed beach response; thus, a site-specific calibration was needed. XBeach was calibrated by applying a two-step approach. The first step was to increase the parameterized wave asymmetry sediment transport component (the *facua* parameter in model input). A higher value resulted in less net offshore sediment transport and in superior calibration. The second step was to increase the bed roughness.

The validation process focused on three cross-shore profiles. The difference between the pre- and post-storm profiles reflect the morphological changes that took place on the beach as a result of the extreme event. The results of the calibrated model were evaluated by comparing the results with measured in-situ pre-storm and post-storm profiles in terms of the Brier Skill Score (BSS) (Sutherland et al., 2004; Bugajny et al., 2013), which is a commonly used statistical indicator for the evaluation of morphological models:

$$BSS = 1 - \left(\frac{\langle |x_p - x_m|^2 \rangle}{\langle |x_b - x_m|^2 \rangle}\right) \quad (8)$$

where x_p is the predicted profile from XBeach; x_m is the measured profile (post-storm) and x_b is the initial (pre-storm) profile. The BSS classification states that BSS < 0, bad; 0 – 0.3, poor; 0.3 – 0.6, reasonable/fair; 0.6 - 0.8, good; and 0.8 – 1.0, excellent. The verification of the modeling results was carried out on the basis of BSS value for each profile. Since there was no bathymetry data available for the study area just before and immediately after Hurricane Irene (August 2011), the measured bathymetries for the month of April 2011 (before the storm) and October 2011 (after the storm) were used. The April 2011 measurements were used as the initial

bathymetry input and the model was run for five days (25-29 August). The resultant cross-shore profile was then compared to the in-situ data measured in October 2011. Validation focused on the eastern end of the study area, as it experiences the most erosion.

Fig. 13 presents the location of the transects used for model validation and assessment of future erosion. Profile 1 is located between two breakwaters on the eastern end of East Ocean View Beach and shows a good BSS score of 0.42. Profile 2 is representative of the central part of East Ocean View and has a BSS score of 0.11. Profile 3 in central Ocean View crosses a breakwater and has a BSS score of 0.33. This profile was specifically taken into consideration to determine the behavior of sediments around a breakwater. Table (6) summarizes the BSS values for the three profiles. Even though the calculated profiles don't deviate much from the measured post-storm profiles which can be seen in Fig. 14, the overall model performance is acceptable but not excellent, especially for Profile 2. This might be attributed to the fact that the beach doesn't experience significant erosion during the storm and thus, the BSS formula becomes extremely sensitive to even the slightest deviation from the measured values. Some studies that don't demonstrate an acceptable point-by-point comparison between XBeach and profile measurements (e.g. Bugajny et al., 2013; Pender and Karunarathna, 2012; Sanuy and Jiménez, 2019) show good BSS values because the erosion is high for their modeled storm event. This allows the modeled profiles to have higher deviation from the measured profiles and still have decent BSS values. All in all, our model did perform well for two profiles and, thus, was used for further analysis.

Table 6. Brier Skill Score (BSS) for three cross-shore profiles.

Profiles	1	2	3
Brier Skill Score (BSS)	0.42	0.11	0.33

Fig. 13 Location of cross-shore profiles used for XBeach model validation.

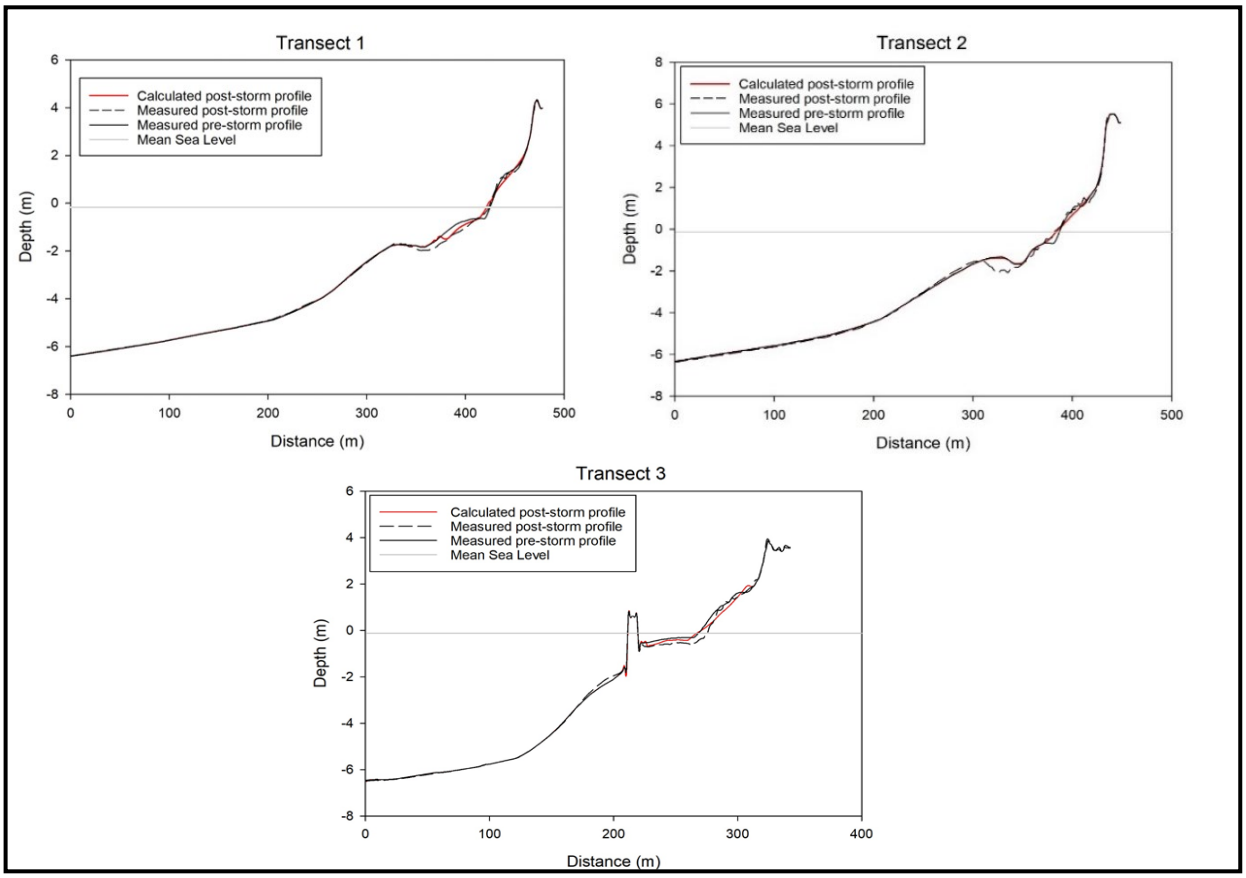

Fig. 14 Comparison of calculated profile vs measured pre and post storm profiles for the three cross-shore profiles.

5.2 Water Level and Significant Wave Height under Future RSLR Scenarios

Time-series of water level and 2D wave spectra from the coupled FLOW+WAVE model were used as boundary conditions for the XBeach model. Hence, it is informative to investigate the variation of these parameters for different RSLR scenarios along the XBeach model boundary and assess their correlation with the modeled erosion. The maximum water level and the maximum significant wave height given by the hydrodynamic+wave model for each RSLR scenario was plotted at the seaward extent of the three transects used for XBeach validation. Fig. 15(a) shows that RSLR varies maximum water level along the XBeach boundary uniformly and in an increasing nonlinear manner. However, maximum significant wave height exhibits significant variation along the boundary (Fig. 15(b)). The increase in maximum water level and maximum significant height for different RSLR scenarios, compared to the 2011 baseline scenario, has been detailed in Table (7).

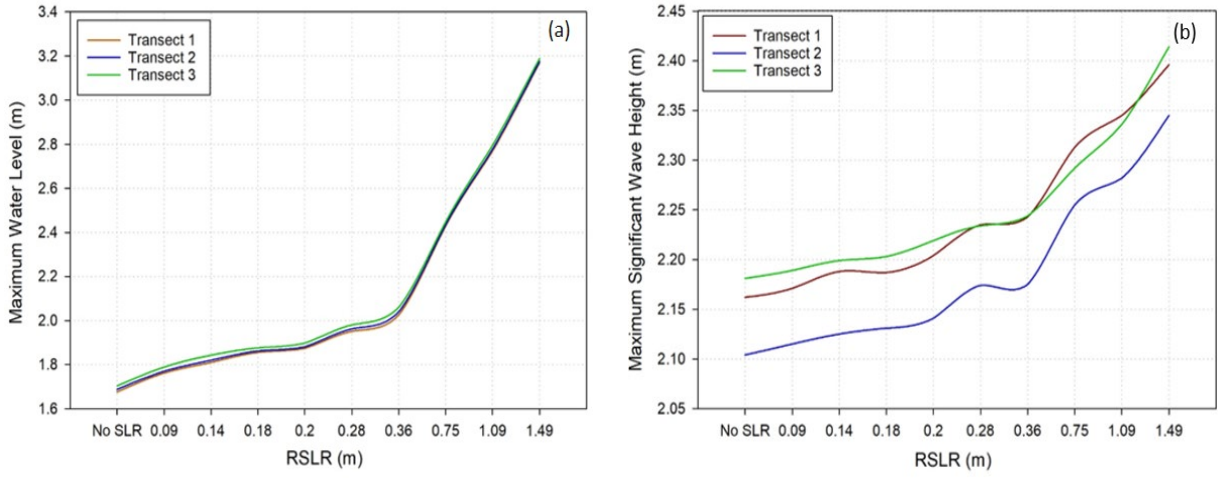

Fig. 15 Variation of hydrodynamics with RSLR at offshore boundary of the XBeach transects (a) Maximum Water Level variation (b) Maximum Significant Wave Height variation.

Table 7. Increase in maximum water level and significant wave height from 2011 at the boundary of each transect for 3 RSLR scenarios.

Parameter	Transect	2020 H=0.18 m RSLR	2030 H=0.36 m RSLR	2070 H=1.49 m RSLR
Increase in Maximum Water Level (m)	Transect 1	0.18	0.349	1.494
	Transect 2	0.174	0.351	1.488
	Transect 3	0.172	0.356	1.485
Increase in Maximum Significant Wave Height (m)	Transect 1	0.025	0.081	0.234
	Transect 2	0.027	0.071	0.241
	Transect 3	0.022	0.063	0.233

5.3 Erosion under Future RSLR Scenarios

Model results show that sea level rise clearly increases the impact of the storm event on shoreline erosion. Summation of erosion/accretion along a transect gives the net volume eroded in terms of meters (m^3/m^2). Volume eroded along each transect was calculated for the 9 RSLR scenarios and was plotted (Fig. 16). Table (8) shows the erosion for the three model years for the high RSLR scenario along the transects. The combination of increased sea level and wave height almost doubles the erosion in 2070 for a Hurricane Irene-like event with high RSLR. Transects 1 and 3 experience an increase in erosion by 2.59 m and 5.93 m, respectively. Even Transect 2, that doesn't have a high BSS value, shows a similar pattern, indicating a doubled erosion volume.

Table 8. Calculated erosion in m (m^3/m^2) along the transects for the 3 high RSLR scenarios for the 3 model years.

RSLR scenario	Transect 1	Transect 2	Transect 3
2011 No SLR	1.91	1.10	6.57
2020 H = 0.18 m	2.30	1.24	7.17
2030 H = 0.36 m	2.62	1.12	7.67
2070 H = 1.49 m	4.50	1.85	12.50

The XBeach simulation results also show that erosion is concentrated very close to the mean sea level, between -2 to 0 m depth. This finding is noteworthy, as it indicates that the area where most of the erosion is concentrated, elevates with increasing sea level. It can be concluded that waves progressively break further upland as sea level rises and, thus, higher elevations of the transect experience intensified erosion. Fig. 17 shows the location of the erosion hotspot along Transect 3 for the baseline case and two RSLR scenarios. For 2011, beach erosion mainly occurs after the toe of the breakwater. However, in 2070, under moderate RSLR of 0.75 m, the waves cause erosion of the subaerial part of the beach, whereas, under high RSLR of 1.49 m, the dune gets eroded.

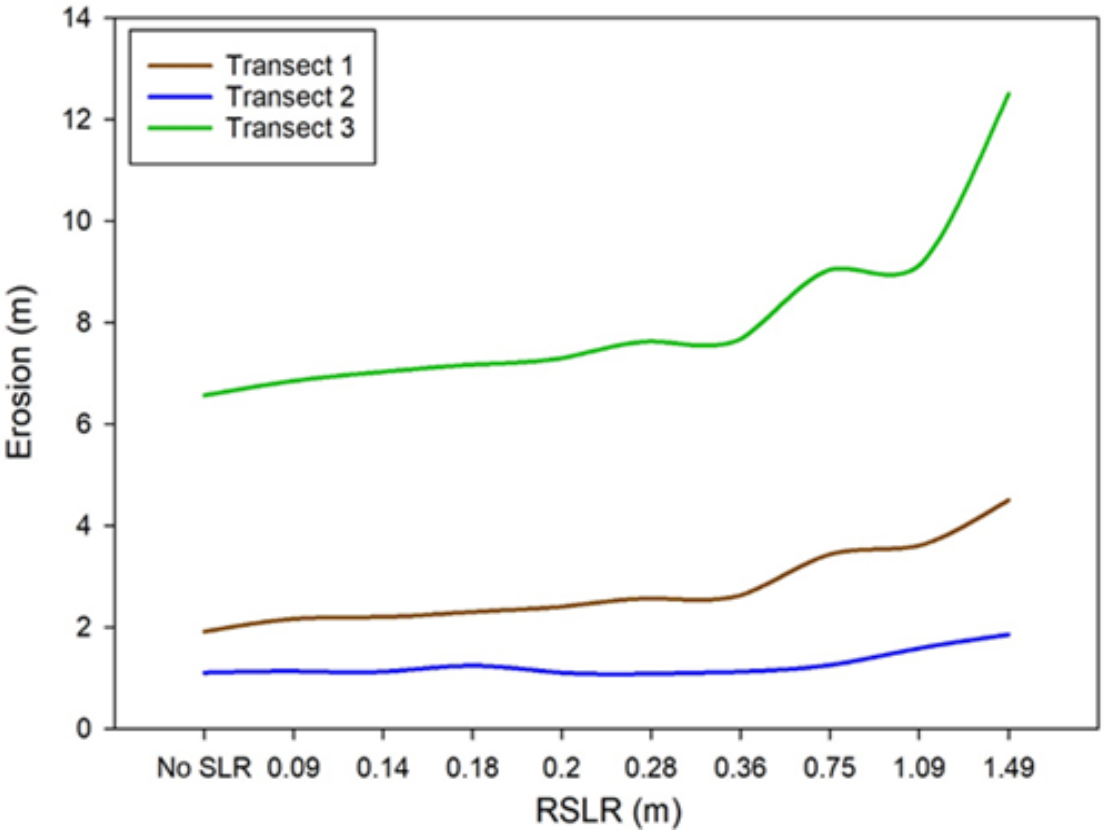

Fig. 16 Plot of erosion in m (m^3/m^2) along the three transects for the 9 RSLR scenarios.

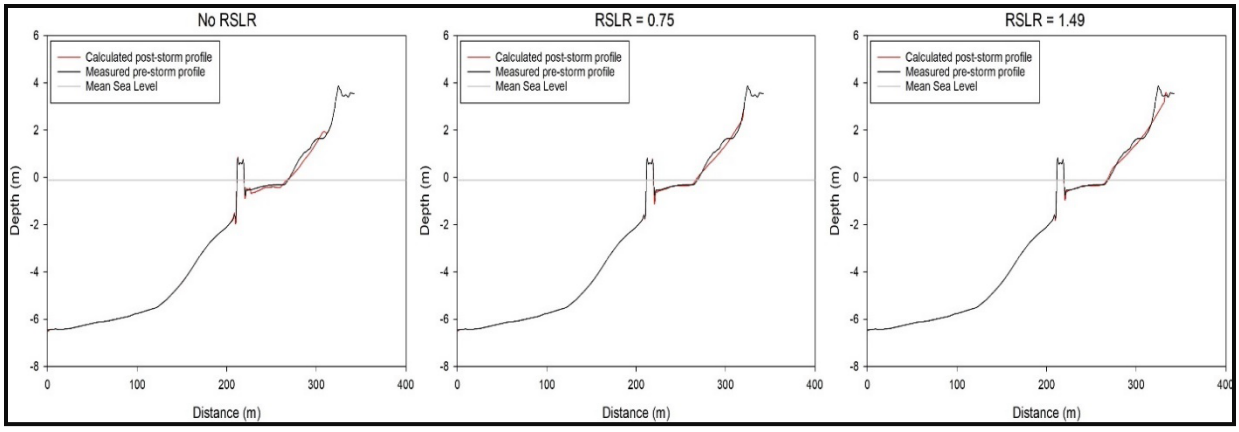

Fig. 17 Variation of erosion hotspot along Transect 3 for baseline case and two RSLR scenarios.

5.4 Shoreline Recession under Future RSLR Scenarios

Shoreline recession refers to the landward shift of the coastline position. The two causes of shoreline recession are sediment loss and an increase in sea levels. Shoreline recession was calculated for scenarios that would increase the future sea level significantly compared to the baseline 2011 scenario. With 2020 almost upon us, studying shoreline recession for it is not of much use and, thus, our focus was more towards the future 2030 and 2070 scenarios. Five RSLR scenarios were selected, i.e., 2030 (H), 2070 (M), 2070 (IH), 2070 (H), and shoreline recession was calculated and tabulated in Table (9). Shoreline recession was calculated by measuring the additional length of the beach that would be submerged under the future sea level, compared to the present shoreline position. Fig. 18 shows the shoreline recession for the 2070 (H) RSLR scenario. Here, shoreline recession is the sum of shoreline retreat due to inundation and erosion. Transect 2, which experiences the least erosion among the three transects, experiences more shoreline recession than Transect 1 and, in some RSLR cases, than even Transect 3. This is attributed to the gentle slope of Transect 2 compared to Transects 1 and 3. Gentle slope leads to more inundation and, thus, causes higher shoreline recession.

Table 9. Shoreline recession in meters at the three transects for five RSLR scenarios.

Transect	2030 H = 0.36 m RSLR	2070 M = 0.75 m RSLR	2070 IH=1.09 m RSLR	2070 H=1.49 m RSLR
Transect 1	3.5	10	14.5	21.5
Transect 2	13	17	20	27
Transect 3	9.5	19	28	34.5

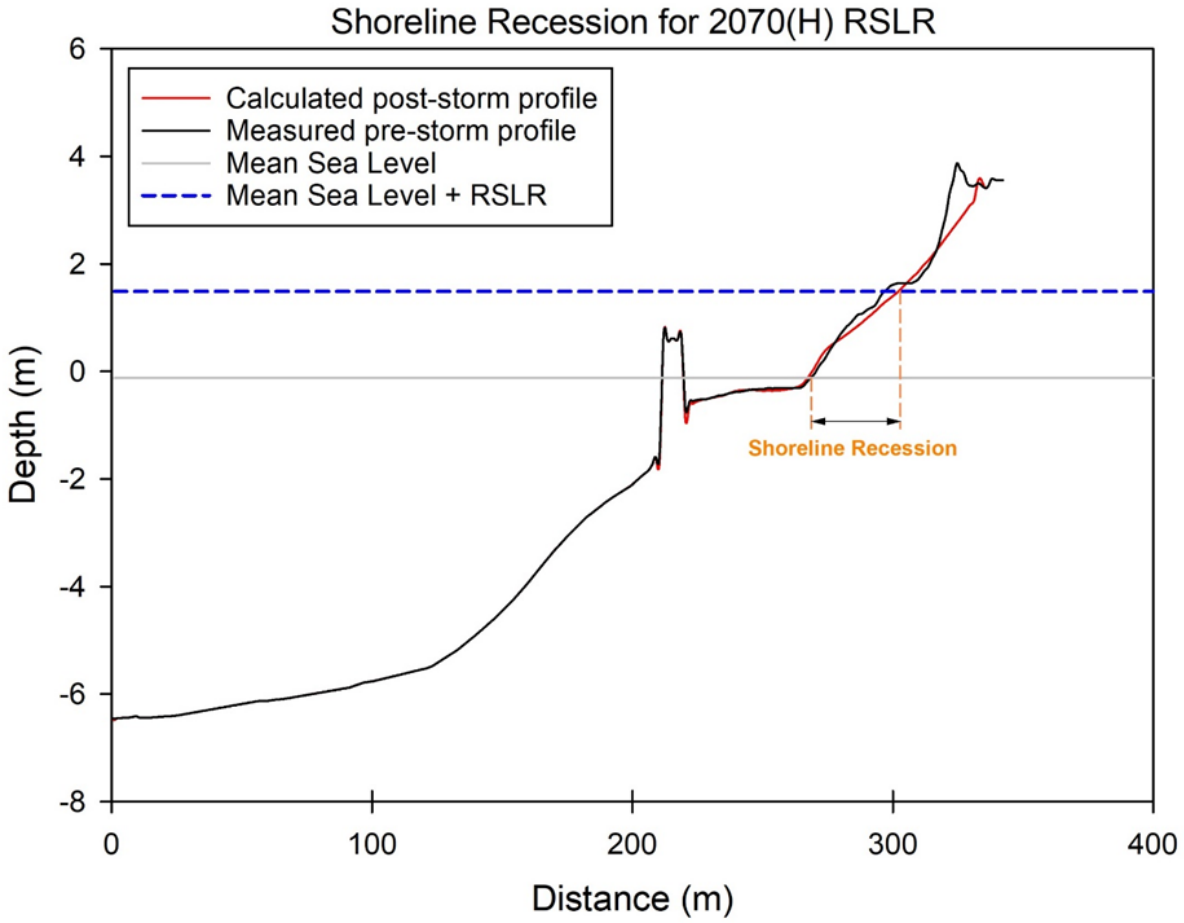

Fig. 18 Shoreline recession at Transect 3 for the year 2070 due to storm induced erosion and high (H) RSLR.

CHAPTER 6

CONCLUSIONS AND DISCUSSION

In this study, the combined effects of a hurricane event and RSLR on a sandy beach were numerically simulated. The study site included the Willoughby Spit and Ocean View shoreline located at the southern shoreline of the Chesapeake Bay and the northern most portion of the city of Norfolk, Virginia. The study focused on this particular area due to its vulnerability to extreme events, high rate of relative sea level rise, and its importance to the community. The Willoughby Spit-Ocean View Beach experiences wave heights on the order of 2-3 m during storm events (USACE, 2014).

To conduct the study, a physics-based predictive modeling framework containing three computational models was developed for sediment transport and shoreline erosion in response to the Hurricane Irene storm event. Delft3D-FLOW and Delft3D-WAVE were dynamically coupled for calculation of hydrodynamic parameters. Two grids were set up in domain decomposition mode for the FLOW model and in one-way nesting mode for the WAVE model. The resolution of the large grid was 125 x 200 m^2, while the resolution of the nested grid was 10 x 10 m^2. The models were run on a cluster that has 2 Intel(R) Xeon(R) Gold 6148 CPUs, with a processing speed of 2.4GHz for each node. During the model run, the two modules of the coupled system used different number of processing cores, based on their specific limitations. Delft3D-FLOW only used 2 cores, one each for the two domains, since domain decomposition does not support parallel computation, whereas Delft3D-WAVE used 40 cores. The computational time for this coupled system was around 6-8 days for one run. The output parameters obtained from this coupled system were then used as boundary conditions for the

XBeach model that calculated the erosion. XBeach calculation was performed on a high-resolution 2D curvilinear grid with cross-shore(dx) and alongshore(dy) grid size ranging from 1-3 m, and the computational time was between 8-9 hours using 600 cores of the same machine. The framework was calibrated and validated with existing in-situ measurements of wave, tides, and bathymetric/topographic cross-shore surveys. It can be asserted that the XBeach model's accuracy was satisfactory and that the results obtained gave a sound basis for estimation of coastal erosion. Three different RSLR scenarios, namely medium (M), intermediate-high (IH) and high (H), each for 2020, 2030, 2070, were then imposed on the baseline model, and shoreline erosion was evaluated for each of them.

The graphs in Fig. 15 and Fig. 16 show the variation of the hydrodynamic parameters and the beach erosion, respectively, under different RSLR scenarios for the three XBeach transects. Increase in RSLR from 2011 to 2070 (H) scenario, showed a non-linear increase in water level. For Transect 1, it increased by 1.494 m, for Transect 2 by 1.488m, and for Transect 3 by 1.485 m. Another observation for the same RSLR scenario was an increase in significant wave height by more than 0.2 m. The combination of increased sea level and wave height almost doubles the erosion in 2070 for a Hurricane Irene-like event with high RSLR. Transects 1 and 3 experience increases in erosion by 2.59 m (m^3/m^2) and 5.93 m (m^3/m^2), respectively. Furthermore, an increase in sea level shifts the area with notable erosion further inland, such that the dune gets eroded under the 2070 (H) RSLR scenario.

Shoreline recession due to increase in sea level and sediment loss was evaluated for the three transects. Table (9) shows the values by which the shoreline would recede under different RSLR scenarios for a Hurricane Irene-like event. Transect 2, which experiences the least erosion among the three transects, has more shoreline recession than Transect 1 and, in some RSLR

cases, even more than Transect 3. This is attributed to the gentle slope of Transect 2. Gentle slope leads to more inundation and, thus, causes higher shoreline recession.

It is notable that Hurricane Irene didn't cause significant erosion at the beach, which is evident from the difference between the pre- and post-storm in-situ data and the simulated erosion values for the baseline case. This might be due to two factors, i.e., the intensity (wave field) and the duration of the storm. Hurricane Irene had a relatively low value of maximum significant wave height, compared to Hurricane Isabel that generated a maximum significant wave height of 3.65 m at Willoughby and that caused major erosion (USACE, 2014). The reader should note that the exact location of this measurement was not available. The Nor'easter of 2009, which had a maximum wave height similar to that of Hurricane Irene (2.5 m at the AWAC gauge location), also caused more erosion because of its longer duration. The Nor'easter produced wave heights greater than a meter for three days continuously, whereas Irene produced wave heights more than 1 m for only one day. This small erosion rate significantly reduced the sensitivity of the model to parameters and made the calibration challenging, as demonstrated by relatively low BSS values for the profiles that were used for validation. In comparison, similar studies that have been conducted in other locations around the world generally have storm conditions with higher wave heights and longer duration. Thus, it can be inferred that Hurricane Irene is probably not the best case to use in studying erosion at the study area. However, the modeling framework performed well despite low erosion.

CHAPTER 7

RECOMMENDATIONS

Many hurdles had to be overcome in order to successfully implement an efficient and accurate modeling system. These challenges include understanding uncertainties in input data, availability of in-situ data with desirable spatiotemporal coverage, and model limitations. Model accuracy depends upon reliable downscaling of hydrodynamic and wave conditions from basin-wide to near-shore scale, and further onshore. Although the models performed well, several steps can be taken to improve them further.

Wave model predictions were very sensitive to accuracy of the wind forcing data. Although the model performed well to predict the overall spatial variability of the wave field, the mean wave direction values near the shore deviated slightly from the measured buoy data. Efforts could be made to improve the values in future through a detailed calibration study.

XBeach underpredicted the erosion values which could be attributed to several factors. Homogeneous sediment size had to be used due to the unavailability of sediment size distribution, which affected the accuracy of simulations. In reality, sediment size varies along and across the coast, as well as vertically through the bed. To improve erosion modeling, field measurements could be carried out to have a better understanding of the sediment size distribution for the sub-aerial, as well as the sub-aqueous parts of the beach. Apart from this, field surveys regarding the vertical variability of sediment composition with depth could also be performed to identify the depth of the non-erodible bed at the beach. Furthermore, there were uncertainties about the exact dimension of coastal structures, namely groins, offshore breakwaters, and outfalls, and their impact on sediment erosion/accretion in their vicinity. Therefore, it is important that the original design, as well as modifications made to the structures

since implementation, be identified and incorporated in the XBeach model. Additionally, the post-storm survey used in the study was conducted several months after the storm; thus, the beach morphology immediately after the storm, that corresponded to model simulations, was not known. Thus, post-storm bathymetric/topographic surveys will be invaluable for future calibration and validation purposes. It is also noted that there are no wave buoys close to the shoreline which could have been used for validation of the nearshore wave parameters calculated by the XBeach model.

For this study, we considered dune erosion only in response to a storm's hydrodynamic forces, i.e. waves and currents whereas aeolian transport can play a substantial role in dune evolution. Coupling a model for coastal processes with one for aeolian transport will provide a comprehensive tool for dune evolution and could be a topic for future research.

REFERENCES

Atkinson, J., J. M. Smith and C. Bender (2013). "Sea-Level Rise Effects on Storm Surge and Nearshore Waves on the Texas Coast: Influence of Landscape and Storm Characteristics." Journal of Waterway, Port, Coastal, and Ocean Engineering **139**(2): 98-117.

Banas, N. S., P. MacCready and B. M. Hickey (2009). "The Columbia River plume as cross-shelf exporter and along-coast barrier." Continental Shelf Research **29**(1): 292-301.

Baptista, A. M., Y. Zhang, A. Chawla, M. Zulauf, C. Seaton, E. P. Myers Iii, J. Kindle, M. Wilkin, M. Burla and P. J. Turner (2005). "A cross-scale model for 3D baroclinic circulation in estuary–plume–shelf systems: II. Application to the Columbia River." Continental Shelf Research **25**(7): 935-972.

Bender, M. A., T. R. Knutson, R. E. Tuleya, J. J. Sirutis, G. A. Vecchi, S. T. Garner and I. M. Held (2010). "Modeled Impact of Anthropogenic Warming on the Frequency of Intense Atlantic Hurricanes." Science **327**(5964): 454-458.

Bilskie, M. V., S. C. Hagen, S. C. Medeiros and D. L. Passeri (2014). "Dynamics of sea level rise and coastal flooding on a changing landscape." Geophysical Research Letters **41**(3): 927-934.

Bird, E. C. F. (1985). "Coastline changes". New York, Wiley & Sons.219

Bolle, A., P. Mercelis, D. J. A. Roelvink, P. Haerens and K. Trouw (2010). "Application and validation of XBeach for three different field sites." Proceedings of the International Conference on Coastal Engineering; No 32 (2010): Proceedings of 32nd Conference on Coastal Engineering, Shanghai, China, 2010.; sediment.40 **1**.

Booij, N., R. Ris and L. Holthuijsen (1999). "A third-generation wave model for coastal regions 1. Model description and validation." Journal of Geophysical Research **104**: 7649-7666.

Bowen, A. J. and D. L. Inman (1969). "Rip currents: 2. Laboratory and field observations." Journal of Geophysical Research (1896-1977) **74**(23): 5479-5490.

Bugajny, N., K. Furmańczyk, J. Dudzińska-Nowak and B. Paplińska-Swerpel (2013). "Modelling morphological changes of beach and dune induced by storm on the Southern Baltic coast using XBeach (case study: Dziwnow Spit)." Journal of Coastal Research **65**(sp1): 672-677, 676.

Castrucci, L. and N. Tahvildari (2018). "Modeling the Impacts of Sea Level Rise on Storm Surge Inundation in Flood-Prone Urban Areas of Hampton Roads, Virginia." Marine Technology Society Journal **52**: 92-105.

Chen, C., R. Beardsley and G. Cowles (2006). "An Unstructured-Grid Finite-Volume Coastal Ocean Model (FVCOM) System." Oceanography **19**: 78–89.

de Winter, R. C., F. Gongriep and B. G. Ruessink (2015). "Observations and modeling of alongshore variability in dune erosion at Egmond aan Zee, the Netherlands." Coastal Engineering **99**: 167-175.

Deltares (2014). "Delft3D-FLOW : Simulation of multi-dimensional hydrodynamic flows and transport phenomena, including sediments User Manual", Version: 3.05.34160, Delft, Netherlands

Deltares (2014). "DELFT3D-WAVE : Simulation of short-crested waves with SWAN User Manual", Version: 3.15.34158, Delft, Netherlands

Dietrich, J. C., M. Zijlema, J. J. Westerink, L. H. Holthuijsen, C. Dawson, R. A. Luettich, R. E. Jensen, J. M. Smith, G. S. Stelling and G. W. Stone (2011). "Modeling hurricane waves and storm surge using integrally-coupled, scalable computations." Coastal Engineering **58**(1): 45-65.

Dingemans, M. W. (1997). "Water Wave Propagation Over Uneven Bottoms"

Egbert, G. D. and S. Y. Erofeeva (2002). "Efficient Inverse Modeling of Barotropic Ocean Tides." Journal of Atmospheric and Oceanic Technology **19**(2): 183-204.

Elias, E. P. L., G. Gelfenbaum and A. J. Van der Westhuysen (2012). "Validation of a coupled wave-flow model in a high-energy setting: The mouth of the Columbia River." Journal of Geophysical Research: Oceans **117**(C9).

Elkan, P., L. Krynock, N. Vanderbeke, J. White and L. Rosenberg (2007). Performance of Beach Fill and Nearshore Breakwaters at East Ocean View Beach, Norfolk, VA. Coastal Sediments '07**:** 2402-2417.

Emanuel, K. A. (1987). "The dependence of hurricane intensity on climate." Nature **326**(6112): 483-485.

Emanuel, K. A. (2008). "The Hurricane—Climate Connection." Bulletin of the American Meteorological Society **89**(5): ES10-ES20.

Enríquez, A. R., M. Marcos, A. Álvarez-Ellacuría, A. Orfila and D. Gomis (2017). "Changes in beach shoreline due to sea level rise and waves under climate change scenarios: application to the Balearic Islands (western Mediterranean)." Nat. Hazards Earth Syst. Sci. **17**(7): 1075-1089.

Feddersen, F. and R. T. Guza (2003). "Observations of nearshore circulation: Alongshore uniformity." Journal of Geophysical Research: Oceans **108**(C1): 6-1-6-10.

Feng, H., D. Vandemark, Q. Yves, C. Bertrand and B. Beckley (2006). "Assessment of wind-forcing impact on a global wind-wave model using the TOPEX altimeter." Ocean Engineering (0029-8018) (Elsevier), 2006-08 , Vol. 33 , N. 11-12 , P. 1431-1461 **33**.

FitzGerald, D. M., M. S. Fenster, B. A. Argow and I. V. Buynevich (2008). "Coastal Impacts Due to Sea-Level Rise." Annual Review of Earth and Planetary Sciences **36**(1): 601-647.

Galappatti, G. and C. B. Vreugdenhil (1985). "A depth-integrated model for suspended sediment transport." Journal of Hydraulic Research **23**(4): 359-377.

Hagen, S. and P. Bacopoulos (2012). "Coastal Flooding in Florida's Big Bend Region with Application to Sea Level Rise Based on Synthetic Storms Analysis." Terrestrial, Atmospheric and Oceanic Sciences **23**: 481.

Hagen, S., J. Westerink, R. Kolar and O. Horstmann (2001). "Two-dimensional, unstructured mesh generation for tidal models." International Journal for Numerical Methods in Fluids - INT J NUMER METHOD FLUID **35**: 669-686.

Hardaway, C., D. A. Milligan, L. M. Varnell, C. A. Wilcox, G. R. Thomas and T. R. Comer (2005). "Shoreline Evolution Chesapeake Bay Shoreline City of Norfolk, VA", Virginia Institute of Marine Science

Harter, C. and J. Figlus (2017). "Numerical modeling of the morphodynamic response of a low-lying barrier island beach and foredune system inundated during Hurricane Ike using XBeach and CSHORE." Coastal Engineering **120**: 64-74.

Hasselmann, K., T. Barnett, E. Bouws, H. Carlson, D. Cartwright, K. Enke, J. Ewing, H. Gienapp, D. Hasselmann, P. Kruseman, A. Meerburg, P. Muller, D. Olbers, K. Richter, W. Sell and H. Walden (1973). "Measurements of wind-wave growth and swell decay during the Joint North Sea Wave Project (JONSWAP)." Deut. Hydrogr. Z. **8**: 1-95.

Hopkins, J., S. Elgar and B. Raubenheimer (2016). "Observations and model simulations of wave-current interaction on the inner shelf." Journal of Geophysical Research: Oceans **121**(1): 198-208.

Hummel, S. and E. D. de Goede (2000). Domain decomposition with grid refinement for shallow water modeling. 4th International Conference on Hydroinformatics, Iowa City, USA, Iowa Institute of Hydraulic Research.

Irish, J. L., A. E. Frey, M. E. Mousavi, F. Olivera, B. L. Edge, J. Kaihatu, L. M. Dunkin and Y. K. Song (2009). Predicting the influence of climate change on hurricane flooding. Coastal Engineering 2008**:** 1050-1059.

Janssen, P. A. E. M. (1989). "Wave-Induced Stress and the Drag of Air Flow over Sea Waves." Journal of Physical Oceanography **19**(6): 745-754.

Lindemer, C., N. Plant, J. A. Puleo, D. Thompson and T. Wamsley (2010). "Numerical simulation of a low-lying barrier island's morphological response to Hurricane Katrina." Coastal Engineering **57**: 985–995.

Liu, Y., P. MacCready and B. M. Hickey (2009). "Columbia River plume patterns in summer 2004 as revealed by a hindcast coastal ocean circulation model." Geophysical Research Letters **36**(2).

Luettich, J. R., J. Westerink and N. Scheffner (1992). "ADCIRC: An Advanced Three-Dimensional Circulation Model for Shelves, Coasts, and Estuaries. Report 1. Theory and Methodology of ADCIRC-2DDI and ADCIRC-3DL." Dredging Research Program Tech. Rep. DRP-92-6: 143.

Luijendijk, A. P., R. Ranasinghe, M. A. de Schipper, B. A. Huisman, C. M. Swinkels, D. J. R. Walstra and M. J. F. Stive (2017). "The initial morphological response of the Sand Engine: A process-based modelling study." Coastal Engineering **119**: 1-14.

McCall, R. T., J. S. M. Van Thiel de Vries, N. G. Plant, A. R. Van Dongeren, J. A. Roelvink, D. M. Thompson and A. J. H. M. Reniers (2010). "Two-dimensional time dependent hurricane overwash and erosion modeling at Santa Rosa Island." Coastal Engineering **57**(7): 668-683.

Mei, C. (1983). "The applied dynamics of ocean surface waves". New York, Wiley

Mousavi, M. E., J. Irish, A. Frey, F. Olivera and B. Edge (2011). "Global Warming and Hurricanes: The Potential Impact of Hurricane Intensification and Sea Level Rise on Coastal Flooding." Climatic Change **104**: 575-597.

Mulligan, R. P., A. E. Hay and A. J. Bowen (2008). "Wave-driven circulation in a coastal bay during the landfall of a hurricane." Journal of Geophysical Research: Oceans **113**(C5).

Mulligan, R. P., A. E. Hay and A. J. Bowen (2010). "A wave-driven jet over a rocky shoal." Journal of Geophysical Research: Oceans **115**(C10).

NOAA. (2019). "What percentage of the American population lives near the coast?" Retrieved 11/03/2019, 2019, from https://oceanservice.noaa.gov/facts/population.html.

Passeri, D. L., M. V. Bilskie, N. G. Plant, J. W. Long and S. C. Hagen ((2018)). "Dynamic modeling of barrier island response to hurricane storm surge under future sea level rise." Climatic Change **149**(3): 413-425.

Passeri, D. L., S. C. Hagen, S. C. Medeiros, M. V. Bilskie, K. Alizad and D. Wang (2015). "The dynamic effects of sea level rise on low-gradient coastal landscapes: A review." Earth's Future **3**(6): 159-181.

Pender, D. and H. Karunarathna (2012). "Modeling beach profile evolution - A statistical-process based approach." Coastal Engineering Proceedings **1**.

Ranasinghe, R., C. Swinkels, A. Luijendijk, D. Roelvink, J. Bosboom, M. Stive and D. Walstra (2011). "Morphodynamic upscaling with the MORFAC approach: Dependencies and sensitivities." Coastal Engineering **58**(8): 806-811.

Rego, J. L. and C. Li (2009). "On the importance of the forward speed of hurricanes in storm surge forecasting: A numerical study." Geophysical Research Letters **36**(7).

Ris, R. C., L. H. Holthuijsen and N. Booij (1999). "A third-generation wave model for coastal regions: 2. Verification." Journal of Geophysical Research: Oceans **104**(C4): 7667-7681.

Roelvink, D., A. Reniers, A. van Dongeren, J. van Thiel de Vries, R. McCall and J. Lescinski (2009). "Modelling storm impacts on beaches, dunes and barrier islands." Coastal Engineering **56**(11): 1133-1152.

Roelvink, J. A. and G. K. F. M. Van Banning (1995). "Design and development of DELFT3D and application to coastal morphodynamics." Oceanographic Literature Review **42**(11): 925.

Saha, S., S. Moorthi, X. Wu, J. Wang, S. Nadiga, P. Tripp, D. Behringer, Y.-T. Hou, H.-y. Chuang, M. Iredell, M. Ek, J. Meng, R. Yang, M. P. Mendez, H. v. d. Dool, Q. Zhang, W. Wang, M. Chen and E. Becker (2014). "The NCEP Climate Forecast System Version 2." Journal of Climate **27**(6): 2185-2208.

Sanuy, M. and J. A. Jiménez (2019). "Sensitivity of Storm-Induced Hazards in a Highly Curvilinear Coastline to Changing Storm Directions. The Tordera Delta Case (NW Mediterranean)." Water **v. 11**(no. 4): 2019 v.2011 no.2014.

Sebastian, A., J. Proft, J. C. Dietrich, W. Du, P. B. Bedient and C. N. Dawson (2014). "Characterizing hurricane storm surge behavior in Galveston Bay using the SWAN+ADCIRC model." Coastal Engineering **88**: 171-181.

Sherwood, C. R., J. W. Long, P. J. Dickhudt, P. S. Dalyander, D. M. Thompson and N. G. Plant (2014). "Inundation of a barrier island (Chandeleur Islands, Louisiana, USA) during a hurricane: Observed water-level gradients and modeled seaward sand transport." Journal of Geophysical Research: Earth Surface **119**(7): 1498-1515.

Smallegan, S. M., J. L. Irish, A. R. Van Dongeren and J. P. Den Bieman (2016). "Morphological response of a sandy barrier island with a buried seawall during Hurricane Sandy." Coastal Engineering **110**: 102-110.

Smith, J. M., M. A. Cialone, T. V. Wamsley and T. O. McAlpin (2010). "Potential impact of sea level rise on coastal surges in southeast Louisiana." Ocean Engineering **37**(1): 37-47.

Sutherland, J., A. H. Peet and R. L. Soulsby (2004). "Evaluating the performance of morphological models." Coastal Engineering **51**(8): 917-939.

Sweet, W. V., R. E. Kopp, C. P. Weaver, J. Obeysekera, R. M. Horton, E. R. Thieler and C. Zervas (2017). "Global and Regional Sea Level Rise Scenarios for the United States. NOAA Technical Report NOS CO-OPS 083",

Tolman, H. (2009). "User manual and system documentation of WAVEWATCH III version 3.14." Analysis **166**.

USACE (2014). "Hurricane sandy Limited reevaluation report, Willoughby spit and vicinity", Norfolk, VA

Valchev, N., P. Eftimova and N. Andreeva ((2018)). "Implementation and validation of a multi-domain coastal hazard forecasting system in an open bay." Coastal Engineering **134**: 212-228.

Virginia Department of Conservation and Recreation. (2019). Retrieved October 10, 2019, from http://www.dcr.virginia.gov/soil-and-water/seas.

Warner, J., B. Armstrong, R. He and J. Zambon (2010). "Development of a Coupled Ocean-Atmosphere-Wave-Sediment Transport (COASWST) modeling system." Ocean Modelling **35**: 230-244.

Warren, I. R. and H. K. Bach (1992). "MIKE 21: a modelling system for estuaries, coastal waters and seas." Environmental Software **7**(4): 229-240.

Whitham, G. (1974). "Linear and nonlinear waves". New York, Wiley

Xie, L., H. Liu and M. Peng (2008). "The effect of wave–current interactions on the storm surge and inundation in Charleston Harbor during Hurricane Hugo 1989." Ocean Modelling **20**(3): 252-269.

Yin, K., S. Xu, W. Huang and Y. Xie (2017). "Effects of sea level rise and typhoon intensity on storm surge and waves in Pearl River Estuary." Ocean Engineering **136**: 80-93.

Zhang, K., B. C. Douglas and S. P. Leatherman (2004). "Global Warming and Coastal Erosion." Climatic Change **64**(1): 41.

VITA

Akash Sahu was born in Lucknow, Uttar Pradesh, India in 1992. He completed his Bachelor of Technology from Motilal Nehru National Institute of Technology Allahabad, India in Civil Engineering. After that he worked as a Research Assistant at IIT Bombay, India for a year and a half and later moved to the United States of America to pursue a Master of Science in Civil Engineering from Old Dominion University in 2017. With his focus on Coastal Engineering, he joined Dr. Navid Tahvildari's research team and began his graduate studies. He plans to continue working in this field and join a major Civil Engineering firm as a Coastal Engineer or Numerical Modeler.